Stockholm University

Waves and instabilities through the lens of asymptotic analysis

Anthony Bonfils

Doctoral Thesis in Theoretical Physics at Stockholm University, Sweden 2023

Waves and instabilities through the lens of asymptotic analysis

Anthony Bonfils

Academic dissertation for the Degree of Doctor of Philosophy in Theoretical Physics at Stockholm University to be publicly defended on Friday 26 May 2023 at 13.00 in hörsal 3, hus 2, Albano, Albanovägen 18 and online via Zoom, public link is available at the department website.

Abstract

Understanding the interaction of water waves with winds and marine currents is a fundamental problem in geophysical fluid dynamics. From the point of view of hydrodynamic stability, surface waves are regarded as perturbations of an inviscid parallel shear flow modeling the wind in the air and the current in the water. For small two-dimensional perturbations, the linearization of the Euler equation of motion yields an eigenvalue problem to be solved for a given wavenumber k. The eigenfunction is a streamfunction obeying the so-called Rayleigh equation. The eigenvalue is a complex phase speed, c, whose real part is the actual phase speed of sheared waves while the imaginary part of kc is the growth rate of the wave amplitude. Using the smallness of the air/water density ratio and assuming no flow in the water, Miles solved this eigenvalue problem perturbatively in 1957. He uncovered an instability of the wind field due to a critical layer in the air, where the wind speed equals the phase speed of free surface waves, and showed that the growth rate of wind-waves is proportional to the square modulus of the solution of the Rayleigh equation at the critical level. This level is a regular singular point, which makes the resolution of the Rayleigh equation challenging. For that reason, an explicit expression of the growth rate of the Miles instability as a function of the wavenumber was lacking. Firstly, I designed a numerical scheme to solve the Rayleigh equation for an arbitrary monotonic wind profile. Secondly, I solved it analytically using asymptotic methods for long and short waves.

In physical oceanography, a standard model for the mean turbulent wind field is the logarithmic profile, which contains only one length scale: the roughness length, $z_0 \sim 1$ mm, accounting for the presence of waves on the water surface. I am interested in waves propagating due to gravity and surface tension, which have wavelengths ranging from a few millimeters to hundreds of meters. Hence, a natural small parameter is kz_0, which I used to obtain long wave solutions of the Rayleigh equation, and subsequently the growth rate of the Miles instability. The comparison with both numerical and measured growth rates is excellent. Furthermore, I approximated the maximum growth rate in the strong wind limit, and inferred that the fastest growing wave is such that the aerodynamic pressure is in phase with the wave slope.

I also considered the short wave limit of the eigenvalue problem. Using $1/(kL)$ as a small parameter, where L is a characteristic length scale of the shear, I found general asymptotic solutions for interfacial waves in presence of a wind and a current, where the density ratio does not need to be small. One application concerns the mixing of elements at the surface of white dwarfs. Moreover, short wave asymptotics provide insights on another instability. When waves have a phase speed that matches the current speed, there is another critical layer, in the water, which is responsible for the so-called rippling instability. I obtained a general asymptotic formula for the growth rate of this instability.

Finally, I used my experience in solving eigenvalue problems to study, in collaboration with other researchers, wrinkles in thin elastic sheets floating on a liquid foundation. We had to solve a fourth order eigenvalue problem where the eigenvalue is the compressive load imposed on the sheet and the eigenfunction is the vertical displacement. For homogeneous sheets, the bending stiffness of the sheet is constant and the eigenvalue problem could be solved analytically. We found that the buckling shape has a symmetric and an antisymmetric mode. The mode associated with the minimum compressive load depends on the size of the confined sheet. Hence, there are changes of symmetry at certain confinement sizes for which the buckling shape is degenerate. We numerically showed that this degeneracy disappears for composite sheets, whose bending stiffness depends on space due to the presence of liquid inclusions.

Keywords: *waves, wrinkles, instabilities.*

Stockholm 2023
http://urn.kb.se/resolve?urn=urn:nbn:se:su:diva-216397

ISBN 978-91-8014-292-2
ISBN 978-91-8014-293-9

Department of Physics

Stockholm University, 106 91 Stockholm

WAVES AND INSTABILITIES THROUGH THE LENS OF ASYMPTOTIC ANALYSIS

Anthony Bonfils

Stockholm
University

Waves and instabilities through the lens of asymptotic analysis

Anthony Bonfils

ISBN print 978-91-8014-292-2
ISBN PDF 978-91-8014-293-9

Printed in Sweden by Universitetsservice US-AB, Stockholm 2023

This thesis is in honor of
John W. Miles.

Abstract

Understanding the interaction of water waves with winds and marine currents is a fundamental problem in geophysical fluid dynamics. From the point of view of hydrodynamic stability, surface waves are regarded as perturbations of an inviscid parallel shear flow modeling the wind in the air and the current in the water. For small two-dimensional perturbations, the linearization of the Euler equation of motion yields an eigenvalue problem to be solved for a given wavenumber k. The eigenfunction is a streamfunction obeying the so-called Rayleigh equation. The eigenvalue is a complex phase speed, c, whose real part is the actual phase speed of sheared waves while the imaginary part of kc is the growth rate of the wave amplitude. Using the smallness of the air/water density ratio and assuming no flow in the water, Miles solved this eigenvalue problem perturbatively in 1957. He uncovered an instability of the wind field due to a critical layer in the air, where the wind speed equals the phase speed of free surface waves, and showed that the growth rate of wind-waves is proportional to the square modulus of the solution of the Rayleigh equation at the critical level. This level is a regular singular point, which makes the resolution of the Rayleigh equation challenging. For that reason, an explicit expression of the growth rate of the Miles instability as a function of the wavenumber was lacking. Firstly, I designed a numerical scheme to solve the Rayleigh equation for an arbitrary monotonic wind profile. Secondly, I solved it analytically using asymptotic methods for long and short waves.

In physical oceanography, a standard model for the mean turbulent wind field is the logarithmic profile, which contains only one length scale: the roughness length, $z_0 \sim 1$ mm, accounting for the presence of waves on the water surface. I am interested in waves propagating due to gravity and surface tension, which have wavelengths ranging from a few millimeters to hundreds of meters. Hence, a natural small parameter is kz_0, which I used to obtain long wave solutions of the Rayleigh equation, and subsequently the growth rate of the Miles instability. The comparison with both numerical and measured growth rates is excellent. Furthermore, I approximated the maximum growth rate in the strong wind limit, and inferred that the fastest growing wave is such that the aerodynamic pressure is in phase with the wave slope.

I also considered the short wave limit of the eigenvalue problem. Using $1/(kL)$ as a small parameter, where L is a characteristic length scale of

the shear, I found general asymptotic solutions for interfacial waves in presence of a wind and a current, where the density ratio does not need to be small. One application concerns the mixing of elements at the surface of white dwarfs. Moreover, short wave asymptotics provide insights on another instability. When waves have a phase speed that matches the current speed, there is another critical layer, in the water, which is responsible for the so-called rippling instability. I obtained a general asymptotic formula for the growth rate of this instability.

Finally, I used my experience in solving eigenvalue problems to study, in collaboration with other researchers, wrinkles in thin elastic sheets floating on a liquid foundation. We had to solve a fourth order eigenvalue problem where the eigenvalue is the compressive load imposed on the sheet and the eigenfunction is the vertical displacement. For homogeneous sheets, the bending stiffness of the sheet is constant and the eigenvalue problem could be solved analytically. We found that the buckling shape has a symmetric and an antisymmetric mode. The mode associated with the minimum compressive load depends on the size of the confined sheet. Hence, there are changes of symmetry at certain confinement sizes for which the buckling shape is degenerate. We numerically showed that this degeneracy disappears for composite sheets, whose bending stiffness depends on space due to the presence of liquid inclusions.

Sammanfattning

Att förstå växelverkan mellan vattenvågor, vind och havsströmmar är ett grundläggande problem inom geofysisk fluiddynamik. Hydrodynamisk stabilitet kan förstås genom att betrakta ytvågor som störningar, där ett ickevisköst parallell skjuvflöde modellerar vinden i luften och strömmningen i vattnet. För små tvådimensionella störningar, ger en linjarisering av Eulers ekvationer ett egenvärdesproblem som skall lösas för givet vågnummer k. Egenfunktionen är en strömmningsfunktion som uppfyller den så-kallade Rayleigh-ekvationen. Egenvärdet är en komplex fashastighet, c, vars reela del är den faktiska fashastigheten av skjuvvågorna, medan den imaginära delen kc bestämmer hur snabbt vågornas amplitud ökar. Genom att använda att förhållandet mellan tätheterna för luft/vatten är litet, och med antagandet att vattnet inte flödar, lyckades Miles lösa egenvärdeproblemet för små störningar år 1957. Han upptäckte att vindfältet är instabilt på grund av ett kritiskt skikt i luften, där vindhastigheten är lika stor som fashastigheten hos fria ytvågor, och visade att ökningen av vindvågorna är proportionell mot kvadraten på absolutvärdet av lösningarna till Rayleighs ekvation vid den kritiska nivån. Denna nivå är en reguljär singulär punk, viket gör det svårt att lösa Rayleighs ekvationer. Av denna anledning fanns det tidigare inget explicit uttryck för ökningen av Milesinstabiliteten som en funktion av k. Först konstruerade jag ett numeriskt protokoll för att lösa Rayleighs ekvation för en godtycklig monoton vindprofil. Sedan löste jag ekvationen analytiskt genom att använda asymptotiska metoder för långa och korta vågor.

I fysisk oceanografi är en standardmodell för det genomsnittliga turbulenta vindfältet en logaritmitsk profilen, som med endast en, längdskala nämligen grovhetslängden $z_0 \sim 1$ mm, kan förklara förekomsten av vågor på en vattenyta. Jag är intresserad av vågor som propagerar på grund av gravitation och ytspänning, och med våglängder från ett par millimeter upp till hundratals meter. Därför är $kz0$ en natrulig liten parameter som jag använde för att härleda lösningar till Rayleighs ekvation för långa vågor, och sedan tillväxthastigheten för Milesinstabiliteten. Jämförelsen med både numeriska och uppmätta tillväxtshastigheter är utmärkt. Vidare gjorde jag en ungefärlig uppskattning av den maximala tillväxthastigheten för stark vind, och visade att den snabbast växande vågen är sådan att det aerodynamiska trycket är i fas med vågens lutning.

Jag studerade även kortvåggränsen av egenvärdeproblemet. Genom att använda $1/(kL)$ som en liten parameter, där L är enkaraktäristiska längdskala för skjuvningen, fann jag allmänna asymptotiska lösningar för vågor i gränssnittet, i närvaro av vind och en strömning, och där täthetsförhållandet inte nödvändigtvis är litet. En möjlig tillämpning av dessa resultat är mixning av gundämnen vid ytan hos vita dvärgar. Dessutom kan asymptotiska lösningar för korta vågor ge information om ytterligare instabiliteter. När vågor har en fashastighet som matchar strömmens hastighet, så finns ytterligare ett kritiskt lager i vattnet vilket ger upphov till den så-kallade krusningsinstabiliteten. Jag härledde en allmän asymptotisk formel för tillväxthastigheten hos denna instabilitet.

Slutligen använde jag min erfarenhet av att lösa egenvärdeproblem för att, i samarbete med andra forskare, studera skrynklingen i tunna elastiska lager som flyter ovanpå en vätskevolym. Vi var tvungna att lösa ett fjärde gradens egenvärdesproblem där egenvärderna är den kompressiva belastningen på det tunna lagret, och egenfunktionen beskriver den vertikala förskjutningen. För homogena lager är böjstyvheten av lagret konstant, och egenvärdeproblemet kunde lösas analytiskt. Vi fann att bucklingsmoden kan vara symmetriskt eller antisymmetriskt. Lägen som associeras med den minsta kompressiva belastningen beror på storleken av det begränsande lagret. Därför ändras symmetrin vid vissa systemstorlekar för vilka bucklingsmoden är degenererad. Vi visade numeriskt att denna degeneration försvinner för sammansatta lager vars böjstyvhet är lägesberoende på grund av närvaron av vätskeinneslutningar.

We shall go on to the end.
We shall fight in France
We shall fight over the seas and oceans.
We shall fight with growing confidence and growing strength in the air.
We shall defend our island whatever the cost may be
We shall fight on beaches, we shall fight on the landing grounds,
We shall fight in the fields and in the streets,
We shall fight on the hills.
We shall never surrender.

– **Iron Maiden**, *Churchill's Speech*, 1985.

List of Papers

The following papers, referred to in the text by their Roman numerals, are included in this thesis.

PAPER I: **Asymptotic interpretation of the Miles mechanism of wind-wave instability**
A. F. Bonfils, D. Mitra, W. Moon, J. S. Wettlaufer, *J. Fluid Mech.*, **944**, A8 (2022).
DOI: https://doi.org/10.1017/jfm.2022.441

PAPER II: **Flow driven interfacial waves: an asymptotic study**
A. F. Bonfils, D. Mitra, W. Moon, J. S. Wettlaufer, *J. Fluid Mech.*, **submitted** (2023).
DOI: http://arxiv.org/abs/2211.02942

PAPER III: **Wrinkling composite sheets**
M. Suñé, C. Arratia, A. F. Bonfils, D. Vella, J. S. Wettlaufer, *Soft Matter*, **submitted** (2023).
DOI: http://arxiv.org/abs/2303.11460

Author's contribution

The following papers, referred to in the text by their Roman numerals, are included in this thesis.

PAPER I: I performed the numerical and asymptotic resolution of the Rayleigh equation under the guidance of my advisors. I suggested to study the strong wind limit and made the connection with Jeffreys' sheltering hypothesis. I wrote the paper under the guidance of my advisors.

PAPER II: I performed the numerical and asymptotic resolution of the Rayleigh equation under the guidance of my advisors. I suggested to extend the analysis to solve the full eigenvalue problem and worked out the details. I wrote the paper under the guidance of my advisors.

PAPER III: I helped to solve the eigenvalue problem analytically in the case of homogeneous sheets. I found the position of the crossing points. I contributed to the writing of the paper.

Licentiate Thesis contribution

The numerical scheme for solving the Rayleigh equation was described in details in my Licentiate Thesis. I gave a short summary in section 5.3.

Acknowledgements

Si tu ne viens pas à Lagardère, Lagardère ira à toi!
– **Paul Féval**, *Le Bossu*, 1857.

I was six years old when I decided I will be a scientist. At this time, I wanted to be a paleontologist (I learned much later what a physicist is), I wanted to seek exotic stuff and face mysteries of Mother Nature. This has not changed. I am still a victim of my insatiable curiosity and hope I will never be cured from this wonderful disease. When I first met my main advisor, Professor John Wettlaufer, he told me that researcher is the best job in the world. After six years of PhD, including a pandemic, I can only agree with him. I sincerely acknowledge the support from Swedish Research Council Grant 638-2013-9243. However, I have no word to express to John my profound gratitude for giving me the opportunity to realize my childhood dream and helping me to earn my entrance ticket to the world of science. You let me do mistakes until I (almost) stop doing them. You strove to teach me rigor and punctiliousness (I let you judge of whether or not you succeeded). You did your best to civilize my Tarzan English. You made me travel to the New Continent, and walk through lands of Physics and Mathematics that I did not even know existed. I was a larva and you guided my metamorphosis into a nymph; you gave me wings to fly over fluid dynamics, elasticity, geophysics, statistical physics, applied mathematics and probably even beyond, I just do not see it yet. You not only gave me the keys to freedom but also showed me how to make good use of it. Exponential infinite thanks!

Next, many thanks go to my mentor, Thors Hans Hansson, and my other advisors, Dhrubaditya Mitra and Woosok Moon, for their availability, continuous support and wise advice; and thank you Dhruba for trusting me to teach French to your daughter! Huge and warm thanks to my friend and eventually collaborator, Cristobal Arratia, for our numerous in-depth discussions in English or in French; I am so grateful for your kindness and for being always ready to heartily debate scientific and non-scientific questions. Two more persons deserve the title of unofficial advisor: Ralf Eichhorn and Supriya Krishnamurthy. You have always been there for me whenever I needed help, advice or feedback; thank you so much for your generosity. Further thanks to Supriya for trusting me to organize the News and Views. It was a wonderful experience

which helped me to improve my presentation skills and gave me the good habit to read the Physics News!

All along my PhD, Nordita was like a second home for me. I cannot imagine a better place to do a PhD, Nordita is the living utopia of a research institute. I benefited so much from the cohort of fellows and visitors, while the workshops and scientific programs enormously enriched my scientific background. I am very thankful to the Nordita director, Professor Niels Obers, for his help and support during the process of applications for fellowships. The Nordita administration is just amazing. Thanks Elizabeth, Marie and Jimmie for demystifying various bureaucratic issues. Thanks Emina for helping me to make my travel bills. Thanks Hans for having solutions to any technical problem. Thanks Milton for taking care of the kitchen where I had lunch and dinner so many times. I am infinitely grateful to the event team, Olga and Anastasios, for organizing great Fikas, receptions and dinners; I enjoyed every single one until satiety! Along this line, I thank Professor Alexander Balatsky for inviting me several times to events in his group.

Over six years, the Soft Matter group has evolved a lot. I wish to acknowledge all the past and present members for the good moments we had and everything I have learnt from you. I would need a tome to properly thank each of you for what you brought to me, each in a different manner. Special thanks go to Marc Suñé for making me the honor to join his project on wrinkles, without which my future may still have been uncertain. Sincere thanks to Sofia Qvarfort for her effort in the translation of my abstract into Swedish, and to the twins, Sree and Sree, for the many favours they did to me, especially at time of applications. I would have been homeless twice without Stefano Bo and Francesco Coghi; thanks to each of you for lending me your flat. Because food is important in life, spicy thanks to Satyajit, Navaneeth, Sankalp, Vipin, Prabal and Ravi (you don't cook but the spirit is there!) for introducing me to Indian cuisine. Along this line, warm thanks to Mariona and Julia for baking cakes for me. Because sport is as necessary as food to survive to a PhD, strong thanks to Sasha Kyrienko for organizing the Nordita running club and initiating me to bouldering and calisthenics. Good food and intense sport certainly contributed to the completion of my PhD, but not as much as metal. Thus, very harsh thanks to all metal bands for making powerful, sensual and violent music that gave me, in the darkest times, the rage to do the work that had to be done and the strength to hold my engagements. I also thank fantasy writers whose characters walked with me in shadows where no one else could have followed me. Finally, I let a light breeze whisper my thanks to Lisa Eichhorn for her keen mind, our philosophical, societal or metaphysical discussions, and the rhetorical fights where we almost always end up to agree to disagree! Last but not least, I thank my parents for their unconditional love and support.

Contents

List of symbols

$\boldsymbol{\Omega} = \nabla \times \boldsymbol{U}$	Vorticity field of the base state
$\boldsymbol{\omega} = \nabla \times \boldsymbol{u}$	Vorticity field of the perturbation
$\boldsymbol{k} = (k,l)$	Wavenumber vector
$\boldsymbol{U}$	Velocity field of the base state
$\boldsymbol{u} = (u,v,w)$	Velocity field of the perturbation
$\boldsymbol{x} = (x,y,z)$	Position vector
$c_{\min}$	Minimum phase speed
$\mathcal{D} = \frac{d}{dz}$	Vertical derivative
ρ_{a}	Air density
ρ_{w}	Water density
ε	Parameter characterizing the smallness of the perturbation
η	Surface displacement field
γ	Normalized growth rate of the Miles instability
$\hat{\boldsymbol{x}}$	Unit vector in the streamwise direction
$\hat{\boldsymbol{y}}$	Unit vector in the spanwise direction
$\hat{\boldsymbol{z}}$	Unit vector in the vertical direction
$\mathrm{Im}\{\}$	Imaginary part
κ	von Kármán constant
k_{cap}	Capillary wavenumber
$\nabla = (\partial_x, \partial_y, \partial_z)$	Gradient vector
ω	Complex angular frequency
Φ	Velocity potential
ϕ	Streamline displacement

ψ	Streamfunction
$\mathrm{Re}\{\}$	Real part
σ	Surface tension
τ_{w}	Wave-induced Reynolds stress
ζ	Vorticity of the perturbation in 2D
At	Atwood number
Bo	Bond number
c	Complex phase speed
Fr	Froude number
g	Gravitational acceleration
h	Water depth
K	Kinetic energy of the perturbation
P	Pressure field of the base state
p	Pressure field of the perturbation
r	Density ratio
Re	Reynolds number
$s = \mathrm{i}\omega$	Complex growth rate
t	Time
$u_\star$	Friction velocity
U_S	Surface drift
z_0	Roughness length

1. Introduction

You think that you have all the answers for all, in your arrogant way only one way to fall.

– **Iron Maiden**, *Hell on Earth*, 2021.

For centuries, scientists and sailors have been vexed by how the wind and the sea conspire to create the waves upon our oceans [1]. Beyond the fascination that waves exert on observers and the curiosity they arouse in the heart of applied mathematicians, air-sea interaction is an important component of the climate dynamics. The exchanges of heat, moisture and momentum at the air-sea interface indeed have a profound influence on the state of the atmosphere [2]. In particular, drops ejected when waves break are the main source of sea-salt aerosols, which are responsible for clouds formation [3] and thus directly impact the modeling of the hydrological cycle. A deeper understanding of wind-wave growth then appears on the long term as a key to resolve the atmospheric distribution of water vapor — the most potent greenhouse gas — and could ultimately help to assess how fast and how irreversible is Earth's global warming [4].

The wavenumber spectrum of the sea was measured in the sixties by Pierson and Moskowitz [5]. However a theory explaining their observations, in particular the peak of the spectrum, has been lacking. There is a plethora of physical phenomena to distinguish in the life of ocean waves: their generation (a), their propagation (b), their growth (c) and their saturation (d).

(a) Any disturbance of the water surface, for instance due to the motion of a boat or an animal or a falling object, generates perturbations which are known as waves in the common language. When a turbulent wind blows, tiny waves called ripples are created by the advection of eddies across the air-water interface. A resonance mechanism was proposed by Phillips in 1957 [6], and recently confirmed by high resolution direct numerical simulations [7].

(b) Water waves propagate due to restoring forces. Surface tension is responsible for the motion of waves whose wavelength is of order of centimeter, or smaller. Longer waves, with wavelength up to hundreds of meters, propagate via the action of gravity. At even larger scales, the

Coriolis force starts to play a role. In this thesis, we discard the effect of Earth's rotation and focus on waves propagating due to gravity and/or surface tension. The dependence of the phase speed of free surface waves on the wavelength, called the dispersion relation, is known since the XIXth century thanks to Cauchy, Poisson and Airy [8; 9]. However, ocean waves are not free. They are forced by winds while time-dependent anisotropic currents are present in water. Furthermore, the bottom of the sea is not uniform. The temporal and horizontal variations of the medium in which waves propagate lead to refraction effects. Provided that these variations are slow, such effects can be accounted for using ray tracing [10]. The vertical variations require a different framework as they can not only affect the propagation of waves but also make them grow or decay.

We stress that most theories of wave propagation – including ray tracing – are linear, that is they assume waves with an infinitesimal amplitude. Such waves do not propagate any matter: the motion of water particles is purely oscillatory so that the position of an object floating on the water surface does not change. However, for waves of finite amplitude, Stokes showed in 1847 that water particles are also advected at a velocity now known as the Stokes drift. It is extremely important for the transport of nutriments, marine debris, micro-plastics and other pollutants in the ocean. The Stokes drift has been recently calculated from empirical wave spectra but also estimated from satellite measurements [11]. Additionally, the wave-induced Stokes drift can interact with wind-induced shear flows to create the so-called Langmuir circulation. A turbulent flow can raise from this circulation – the so-called Langmuir turbulence – and results in an effective diffusion in the upper ocean layer, which has been investigated using large eddy simulations [12].

(c) Waves rapidly grow as they receive energy from the wind. Although ubiquitous, this energy transfer is still not completely understood. In 1957, Miles [13] averaged the air turbulent fluctuations and represented the wind with a parallel shear flow – a flow whose velocity varies only in the vertical direction. Then, he regarded waves as perturbations of that flow and constructed an inviscid theory to calculate the growth rate of wave energy. He predicted a transfer of energy from wind to waves within a critical layer, located in the air at the height where the wind speed equals the phase speed of free surface waves. The latter is a good approximation to the actual phase speed of waves because the air-water density ratio is small. Although widely studied [14; 15], the theory of Miles still faces a severe technical issue: analytical solutions of the equa-

tion for the stability of the wind – the Rayleigh equation – are available only in very few cases, most of them being unrealistic. In particular, the basic question 'what is the fastest growing wave?' does not have an answer yet. Recent laboratory measurements of the air flow over wind-generated waves provided evidence of the Miles critical layer mechanism [16]. Further evidence were given almost at the same time by fully coupled direct numerical simulations [17].
Within the same framework of stability of a parallel shear flow, an energy transfer from a marine current to waves has also been predicted – a phenomena coined the rippling instability [18]. But, again, the difficulties at solving the Rayleigh equation hinder calculations of the growth rate and phase speed, which in that case can be strongly affected by the shear. Wave growth due to a current has yet to be observed, both in laboratory experiments and in the ocean.

(d) The theory of Miles [13] predicts an exponential growth of the waves due to their interaction with a steady flow. Nonetheless, the wave amplitude cannot grow exponentially forever: the waves should reach at some point a maximum amplitude, characteristic of their saturation, otherwise they break. Only non-linear effects can account for wave saturation. In the sixties, Phillips, Hasselmann and Zakharov independently developed a theory of resonant interactions between water waves [19–21]. The key idea is that two waves (1 and 2) can interact with each other to produce two other waves (3 and 4), provided that they fulfill the resonant condition

$$\boldsymbol{k}_1 + \boldsymbol{k}_2 = \boldsymbol{k}_3 + \boldsymbol{k}_4 \qquad \text{and} \qquad \omega_1 + \omega_2 = \omega_3 + \omega_4, \tag{1.1}$$

where ω_i is the angular frequency of the wave with wavenumber vector $\boldsymbol{k}_i$. The Zakharov equation determines the time evolution of the Fourier amplitude of interacting waves. It has been the object of numerous work, mostly on the wave-wave interaction kernel; the simplest form in date is called the super compact equation [22]. However, the Zakharov equation (or its simplified version) is deterministic and thus not convenient to study a large number of interacting waves, for which a statistical approach would be more useful. This was accomplished in the field of wave turbulence with the wave kinetic equation, which governs the evolution of the wave action $N(\boldsymbol{k},t)$ – the second moment of the wave amplitude divided by the angular frequency [23]. The wave kinetic equation is the wave analogue of the Boltzmann kinetic equations for particle interactions. It has the form

$$\frac{\partial N}{\partial t} = S_{\text{nl}} + S_{\text{in}} + S_{\text{dis}}, \tag{1.2}$$

where S_{nl}, S_{in} and S_{dis} are the non-linear transfer, wind input and dissipation terms, respectively. The non-linear term can be derived from the Zhakarov equation under some (debated) assumptions. The wind input comes from the Miles theory while the dissipation term is phenomenological. The numerical resolution of equation (1.2) is at the heart of current wave forecasts [24]. Recent work bear upon a rigorous derivation of equation (1.2) [25], applications to condensed matter [26] and connections with large deviation theory [27].

In this thesis, we focus on the propagation and the growth of waves. Our goal is to clarify the work of Miles on wind-waves and overcome the technical issues related to the resolution of the Rayleigh equation, in order to finally provide an answer to the basic question 'what is the fastest growing wave?'. Within that framework, we also aim at improving the present results on wave-current interaction, especially the effect of the shear on the phase speed which has been overlooked. Finally, we wish to go beyond surface waves and consider an interface between two fluids whose density ratio is not small. Hence, beyond geophysical motivations, we treat in this thesis a question of fluid mechanics: How do interfacial waves interact with a parallel shear flow? Following Miles, this question can be viewed as a problem of hydrodynamic stability and ultimately reduced to the resolution of an eigenvalue problem. Such a lifting of an environmentally motivated question to mathematical grounds broadens the scope of the concepts and techniques used to solve it. It helps to build a bridge to other areas of continuum mechanics. For instance, another eigenvalue problem arises from the wrinkling of a thin elastic sheet floating on a liquid foundation. The mathematical step from waves to wrinkles and the jump from hydrodynamic to mechanical stability are small. Although the key physical quantities are quite different, in the end only change the order of the differential equation to solve and its boundary conditions. Thus, we used on wrinkles the experience we gained with waves.

We give a short introduction to hydrodynamic stability in chapter 2 in which we define waves and instabilities and show how to reduce a stability question to an eigenvalue problem. In chapter 3, we elaborate on the stability of parallel shear flows, those used to model winds and currents. In particular, we derive the Rayleigh equation and introduce key concepts such as the wave-induced Reynolds stress. Chapter 4 provides some background on interfacial waves. In chapter 5, we review previous work on the interaction of interfacial waves with a parallel shear flow and highlight our contributions. We treat the wind-wave interaction in PAPER I, revisiting the Miles theory and solving the Rayleigh equation asymptotically for long waves. We obtain explicit expressions for the growth rate of wave energy as a function of the wavenumber. In the strong wind limit, we show that the fastest growing wave

has an aerodynamic pressure proportional to the wave slope, in accord with an old hypothesis of Jeffreys [28]. In PAPER II, we solve the general eigenvalue problem for flow driven interfacial waves using short wave asymptotics. We obtain the shear-dependent phase speed of waves for arbitrary wind and current profiles, as well as the growth rates of the Miles and rippling instabilities. We emphasize that the density ratio does not have to be small, which opens a door to astrophysical applications. Finally, we move from fluid dynamics to elasticity in PAPER III, where we calculate the wrinkle pattern and buckling compressive load of a confined elastic sheet floating on a liquid foundation.

Notations:

We use a Cartesian coordinate system with unit vectors $\hat{\boldsymbol{x}}$, $\hat{\boldsymbol{y}}$ and $\hat{\boldsymbol{z}}$ in the streamwise, spanwise and vertical directions, respectively. The position vector is $\boldsymbol{x} = (x, y, z)$ and we use the gradient vector $\nabla = (\partial_x, \partial_y, \partial_z)$.

2. Introduction to hydrodynamic stability

Il faut le malheur pour creuser certaines mines mystérieuses cachées dans l'intelligence humaine ; il faut la pression pour faire éclater la poudre. La captivité a réuni sur un seul point toutes mes facultés flottantes çà et là ; elles se sont heurtées dans un espace étroit ; et, vous le savez, du choc des nuages résulte l'électricité, de l'électricité l'éclair, de l'éclair la lumière.

– **Alexandre Dumas**, *Le Comte de Monte-Cristo*, 1846.

In this chapter, we give the basics of hydrodynamic stability [29; 30]. In section 2.1, we establish the general equations for the velocity and vorticity of a perturbation. Then, we detail the analysis of normal modes in section 2.2, where in particular we define waves and instabilities. All dimensional quantities are denoted with an asterisk *.

2.1 Perturbation of a background flow

Let us consider a homogeneous fluid with density, ρ^*, and kinematic viscosity, ν^*. We want to study the stability of a steady flow, called the base state or the background flow. The velocity and pressure fields are $\boldsymbol{U}^*(\boldsymbol{x}^*)$ and $P^*(\boldsymbol{x}^*)$, respectively. We use the characteristic length scale, L^*, and velocity scale, V^*, to construct dimensionless variables[1] denoted without asterisk. The background flow is incompressible, namely $\nabla\cdot\boldsymbol{U}=0$, and obeys the stationary Navier-Stokes equation:

$$(\boldsymbol{U}\cdot\nabla)\boldsymbol{U} = -\nabla P + Re^{-1}\nabla^2\boldsymbol{U}, \tag{2.1}$$

where $Re\equiv L^*V^*/\nu^*$ is the Reynolds number. For simplicity, we discard any body force. We introduce a small perturbation and write the perturbed fields in the form

$$\boldsymbol{u}_{\rm tot}(\boldsymbol{x},t) = \boldsymbol{U}(\boldsymbol{x}) + \varepsilon\,\boldsymbol{u}(\boldsymbol{x},t) \qquad \text{and} \qquad p_{\rm tot}(\boldsymbol{x},t) = P(\boldsymbol{x}) + \varepsilon\,p(\boldsymbol{x},t), \tag{2.2a,b}$$

[1] The pressure scale is ρ^*V^{*2}.

where 'tot' means 'total' (i.e. base state plus perturbation) and $\varepsilon \ll 1$ characterizes the smallness of the perturbation. We assume that the perturbed flow is still incompressible, that is

$$\nabla \cdot \boldsymbol{u} = 0. \tag{2.3}$$

The perturbed fields are solutions of the time-dependent Navier-Stokes equation,

$$\partial_t \boldsymbol{u}_{\text{tot}} + (\boldsymbol{u}_{\text{tot}} \cdot \nabla)\boldsymbol{u}_{\text{tot}} = -\nabla p_{\text{tot}} + Re^{-1}\nabla^2 \boldsymbol{u}_{\text{tot}}. \tag{2.4}$$

Inserting (2.2*a*,*b*) into equation (2.4) and using the base state equation (2.1), we obtain at order ε

$$(\partial_t + \boldsymbol{U} \cdot \nabla)\boldsymbol{u} + (\boldsymbol{u} \cdot \nabla)\boldsymbol{U} = -\nabla p + Re^{-1}\nabla^2 \boldsymbol{u}. \tag{2.5}$$

Equation (2.5) is linear in $\boldsymbol{u}$, thus much simpler to solve than the original Navier-Stokes equation (2.4).

For the sake of completeness, we now derive the counterpart of equation (2.5) for the vorticity of the perturbation. The base state vorticity is $\nabla \times \boldsymbol{U} \equiv \boldsymbol{\Omega}$. Taking the curl of equation (2.1) governing the base state velocity, we find

$$(\boldsymbol{U} \cdot \nabla)\boldsymbol{\Omega} = (\boldsymbol{\Omega} \cdot \nabla)\boldsymbol{U} + Re^{-1}\nabla^2 \boldsymbol{\Omega}. \tag{2.6}$$

The perturbed vorticity field is

$$\boldsymbol{\omega}_{\text{tot}}(\boldsymbol{x}, t) = \boldsymbol{\Omega}(\boldsymbol{x}) + \varepsilon\, \boldsymbol{\omega}(\boldsymbol{x}, t), \tag{2.7}$$

where $\boldsymbol{\omega} \equiv \nabla \times \boldsymbol{u}$. The time evolution of $\boldsymbol{\omega}_{\text{tot}}$ is governed by the Helmholtz equation[1]:

$$\partial_t \boldsymbol{\omega}_{\text{tot}} + (\boldsymbol{u}_{\text{tot}} \cdot \nabla)\boldsymbol{\omega}_{\text{tot}} = (\boldsymbol{\omega}_{\text{tot}} \cdot \nabla)\boldsymbol{u}_{\text{tot}} + Re^{-1}\nabla^2 \boldsymbol{\omega}_{\text{tot}}. \tag{2.8}$$

Proceeding as for the velocity, we obtain at order ε

$$(\partial_t + \boldsymbol{U} \cdot \nabla)\boldsymbol{\omega} + (\boldsymbol{u} \cdot \nabla)\boldsymbol{\Omega} = (\boldsymbol{\Omega} \cdot \nabla)\boldsymbol{u} + (\boldsymbol{\omega} \cdot \nabla)\boldsymbol{U} + Re^{-1}\nabla^2 \boldsymbol{\omega}. \tag{2.9}$$

Equation (2.9) will be useful in chapter 3.

2.2 Normal modes analysis

Here, the base state is characterized by a single dimensionless number, Re. When external forcing or heating or body forces or interfaces are added into the problem, other dimensionless numbers arise.

[1] We obtain the Helmholtz equation (2.8) by taking the curl of the Navier-Stokes equation (2.4) and using identity (7.5) together with the incompressibility condition (2.3).

2.2.1 Reduction to an eigenvalue problem

The coefficients of equation (2.5) are independent of time. If the background flow has symmetries, those coefficients do not depend on some spatial coordinates. For instance, we consider a base state which is invariant under any horizontal translation, that is $\boldsymbol{U} = \boldsymbol{U}(z)$. Thus, we look for solutions of the form

$$\boldsymbol{u}(\boldsymbol{x},t) = e^{\mathrm{i}(kx+ly)+st}\boldsymbol{f}(z), \qquad k,l,s \in \mathbb{C}. \tag{2.10}$$

Physically, we are studying the perturbation at horizontal scales defined by the wavenumber vector $\boldsymbol{k} = (k,l)$. If k or l have a non-zero imaginary part, the perturbation grows (or decays) exponentially in space. In this work, we assume that $k,l \in \mathbb{R}$ and focus on the time evolution of the perturbation at different scales. Thus, we generally write equation (2.5) as

$$\partial_t \boldsymbol{u} = \mathscr{L}\boldsymbol{u}, \tag{2.11}$$

where $\mathscr{L}$ is a linear differential operator. We insert our ansatz (2.10) into equation (2.11). Transforming differentiation with respect to t, x and y into multiplication by s, $\mathrm{i}k$ and $\mathrm{i}l$ respectively, we obtain

$$\mathscr{L}(\partial_x \to \mathrm{i}k, \partial_y \to \mathrm{i}l)\boldsymbol{f} = s\boldsymbol{f}. \tag{2.12}$$

Hence, s and $\boldsymbol{f}$ are respectively the eigenvalue and vector eigenfunction of the operator $\mathscr{L}$ in Fourier space. The enforcement of boundary conditions in the vertical direction yields a characteristic equation of the form

$$F(s,k,l,Re) = 0. \tag{2.13}$$

Equation (2.13) is a relation between the eigenvalue, s, the streamwise and spanwise wavenumbers, k and l, and the Reynolds number, Re. The Reynolds number is a control parameter. We call normal mode a solution $(\boldsymbol{k},s)$ of equation (2.13) for a fixed value of Re. The temporal stability of a normal mode depends on the real part of s:

(i) If $\mathrm{Re}\{s\} > 0$, the mode is unstable and the perturbation grows exponentially in time. There is an instability.

(ii) If $\mathrm{Re}\{s\} < 0$, the mode is stable and the perturbation decays exponentially in time.

(iii) If $\mathrm{Re}\{s\} = 0$, the mode is neutral.

Evidently, $\mathrm{Re}\{s\}$ is the temporal growth (or decay) rate of the perturbation and strongly depends on the wavenumber vector, $\boldsymbol{k}$. In other words, the perturbation grows (or decays) differently at different scales. The set of possible values for s at a given $\boldsymbol{k}$ is called the spectrum. It may be discrete or continuous.

In general, a base state is perturbed on a broad range of scales so that the entire spectrum of normal modes is excited. All the modes must be stable for the background flow to be stable. Conversely, the background flow is unstable if at least one mode is unstable.

2.2.2 Neutral and marginal stability

A mode is said marginally stable if $\mathrm{Re}\{s\}$ vanishes for a specific value of Re and becomes positive at neighboring values of Re. In particular, we look for the minimum Reynolds number, Re_c, at which a mode is marginally stable. In other words, the background flow becomes unstable when $Re > Re_c$ and the first unstable mode to appear has the wavenumber vector $\boldsymbol{k}_c$. The index 'c' stands for critical. The surface of marginal stability is defined in the space $(\boldsymbol{k}, Re)$ by

$$\mathrm{Re}\{s(\boldsymbol{k}, Re)\} = 0. \tag{2.14}$$

This surface has multiple branches when the spectrum is discrete. It can be shown that the continuous parts of the spectrum do not contribute to flow instability.

A mode is said neutrally stable if $\mathrm{Re}\{s\} = 0$ for a range of values of Re. In that case, the perturbation is a wave. It is a travelling wave if s has a non-zero imaginary part. Otherwise, it is a stationary wave.

For any mode, we define the complex angular frequency by

$$\omega \equiv -\mathrm{i}s. \tag{2.15}$$

If $\mathrm{Re}\{\omega\} \neq 0$, the perturbation travels in the direction defined by $\boldsymbol{k}$ with a phase speed equal to $\mathrm{Re}\{\omega\}/|\boldsymbol{k}|$. We can equivalently work with either s or ω. As our focus is on waves, we find more convenient to use ω. The criteria of stability in terms of the latter are:

(i) If $\mathrm{Im}\{\omega\} > 0$, the mode is unstable and the perturbation grows exponentially in time. There is an instability.

(ii) If $\mathrm{Im}\{\omega\} < 0$, the mode is stable and the perturbation decays exponentially in time.

(iii) If $\mathrm{Im}\{\omega\} = 0$, the mode is neutral.

3. Stability of a parallel shear flow

Point n'est besoin d'espérer pour entreprendre, ni de réussir pour persévérer.
– **Guillaume 1er d'Orange-Nassau, dit le Taciturne** (1533-1584).

In this chapter, we apply the general framework of chapter 2 – with dimensionless variables – to study the stability of a parallel shear flow, $\boldsymbol{U} = U(z)\,\hat{\boldsymbol{x}}$, bounded between $z = z_1$ and $z = z_2$ [29; 31]. We consider a horizontal domain $L_x \times L_y$ with periodic boundary conditions. At the vertical boundaries, we impose a no-slip boundary condition, $\boldsymbol{u} = \boldsymbol{0}$, for a viscous fluid, and a non-penetrative boundary condition, $w = 0$, for an inviscid fluid. We write down the conservation of momentum and energy in sections 3.1 and 3.2, respectively. We derive the Squire theorem in section 3.3, before establishing in section 3.4 the Orr-Sommerfeld and Rayleigh equations for the amplitude of the perturbation's streamfunction. Historical solutions of the Rayleigh equation are derived in section 3.5. Finally, we show in section 3.6 some standard results on the stability of a parallel inviscid flow, including the Rayleigh and Fjørtoft instability conditions.

We let $\boldsymbol{u} = (u, v, w)$ in the Cartesian basis. We also define the horizontal average of a quantity q as

$$\overline{q}(z,t) \equiv \frac{1}{L_x L_y} \int_{-\frac{L_x}{2}}^{\frac{L_x}{2}} \int_{-\frac{L_y}{2}}^{\frac{L_y}{2}} dxdy\; q(x,y,z,t). \tag{3.1}$$

Because of the periodic boundary conditions, we have by construction

$$\overline{\partial_x q} = 0 \qquad \text{and} \qquad \overline{\partial_y q} = 0. \tag{3.2a,b}$$

3.1 Momentum conservation

The incompressible Navier-Stokes equation (2.4) can be written as

$$\partial_t \boldsymbol{u}_{\text{tot}} + \nabla \cdot (\boldsymbol{u}_{\text{tot}} \otimes \boldsymbol{u}_{\text{tot}}) = -\nabla p_{\text{tot}} + Re^{-1} \nabla^2 \boldsymbol{u}_{\text{tot}}. \tag{3.3}$$

The streamwise component is

$$\varepsilon\ \partial_t u + \nabla\cdot\{(U+\varepsilon\ u)\boldsymbol{u}_{\rm tot}\} = -\partial_x p_{\rm tot} + Re^{-1}\nabla^2(U+\varepsilon\ u). \tag{3.4}$$

When averaging equation (3.4), all derivatives with respect to x and y vanish (cf. Eq. 3.2a,b). With the help of the base state equation (2.1), we obtain

$$\varepsilon\ \partial_t\overline{u} + \partial_z\big(\varepsilon\ U\overline{w} + \ \varepsilon^2\ \overline{uw}\big) = \varepsilon\ Re^{-1}\partial_z^2\overline{u}. \tag{3.5}$$

Analogously, averaging the incompressibility condition (2.3) gives $\partial_z\overline{w}=0$. Thus $\overline{w}$ is constant, and must actually be equal to zero because of the boundary conditions. Hence, the local streamwise momentum balance (3.5) becomes

$$\varepsilon\ \partial_t\overline{u} = \varepsilon^2\ \partial_z\tau_{\rm w} + \varepsilon\ Re^{-1}\partial_z^2\overline{u}, \tag{3.6}$$

where we introduced the dimensionless wave-induced Reynolds stress,

$$\tau_{\rm w} \equiv -\overline{uw}. \tag{3.7}$$

Noting that

$$\tau_{\rm w}(z_1,t) = 0 \qquad \text{and} \qquad \tau_{\rm w}(z_2,t) = 0, \tag{3.8a,b}$$

after a vertical integration we find

$$\partial_t\overline{\int_{z_1}^{z_2} dz\ u} = Re^{-1}\big(\partial_z\overline{u}|_{z_2} - \partial_z\overline{u}|_{z_1}\big). \tag{3.9}$$

Therefore, in accord with physical intuition, a viscous parallel flow can only receive or dissipate streamwise momentum through the horizontal boundaries. Moreover, for an inviscid fluid ($Re^{-1}=0$) the mean horizontal momentum of the perturbation is conserved. We note that although this momentum balance is at order ε, it is exact; all high order terms vanished without approximation.

3.2 Energy conservation

With the help of identities (7.1) and (7.2), we write the Navier-Stokes equation for perturbed fields in the form

$$\varepsilon\ (\partial_t + U\partial_x)\boldsymbol{u} + \varepsilon^2\ \nabla\left(\frac{|\boldsymbol{u}|^2}{2}\right) + \varepsilon^2\ \boldsymbol{\omega}\times\boldsymbol{u} + \varepsilon\ w\frac{d\boldsymbol{U}}{dz} = -\varepsilon\ \nabla p - \varepsilon\ Re^{-1}\nabla\times\boldsymbol{\omega}. \tag{3.10}$$

Let

$$K \equiv \frac{|\boldsymbol{u}|^2}{2} \tag{3.11}$$

be the kinetic energy (per unit mass) of the perturbation. A scalar product of equation (3.10) with $\varepsilon\,\boldsymbol{u}$ and the use of identities (7.3) and (7.4) yields

$$\varepsilon^2\,(\partial_t + U\partial_x)K + \nabla\cdot\left\{(\varepsilon^2\,p + \varepsilon^3\,K)\boldsymbol{u}\right\} = -\varepsilon^2\,uw\frac{dU}{dz} + \varepsilon^2\,Re^{-1}\left(\nabla\cdot(\boldsymbol{u}\times\boldsymbol{\omega}) - |\boldsymbol{\omega}|^2\right). \tag{3.12}$$

Next, we take the average defined in equation (3.1) and find

$$\varepsilon^2\,\partial_t\overline{K} + \partial_z\overline{\left\{(\varepsilon^2\,p + \varepsilon^3\,K)w\right\}} = \varepsilon^2\,\tau_{\rm w}\frac{dU}{dz} + \varepsilon^2\,Re^{-1}\left(\partial_z\overline{(\boldsymbol{u}\times\boldsymbol{\omega}\cdot\hat{\boldsymbol{z}})} - \overline{|\boldsymbol{\omega}|^2}\right). \tag{3.13}$$

A vertical integration eventually gives the so-called Reynolds-Orr equation:

$$\partial_t\overline{\int_{z_1}^{z_2} dz\,K} = \int_{z_1}^{z_2} dz\,\tau_{\rm w}\frac{dU}{dz} - Re^{-1}\overline{\int_{z_1}^{z_2} dz\,|\boldsymbol{\omega}|^2}. \tag{3.14}$$

Hence, the rate of change of the mean kinetic energy of the perturbation is equal to the rate of work of the Reynolds stress, plus a term of viscous dissipation which is twice the mean enstrophy of the perturbation. We stress that this energy balance is at order ε^2 and is also exact.

3.3 Squire theorem

In this section, we derive a useful result on the stability of a parallel shear flow: the most unstable mode of the perturbation is longitudinal so that the spanwise component of the perturbation can be discarded. It was derived in 1933 by Squire using an abstract transformation [32]. Here, we take the more physical approach of Lin [33]. We start with equation (2.5), which for a parallel flow simplifies into

$$(\partial_t + U\partial_x)\boldsymbol{u} + w\frac{d\boldsymbol{U}}{dz} = -\nabla p + Re^{-1}\nabla^2\boldsymbol{u}. \tag{3.15}$$

We look for normal modes of a three-dimensional perturbation in the form

$$\boldsymbol{u}(\boldsymbol{x},t) = \mathrm{Re}\left\{\hat{\boldsymbol{u}}(z)\,e^{\mathrm{i}(kx+ly-\omega t)}\right\} \qquad \text{and} \qquad p(\boldsymbol{x},t) = \mathrm{Re}\left\{\hat{p}(z)\,e^{\mathrm{i}(kx+ly-\omega t)}\right\}, \tag{3.16a,b}$$

where $\hat{\boldsymbol{u}} = (\hat{u},\hat{v},\hat{w})$. We let $\mathcal{D} \equiv \frac{d}{dz}$ and recall that $\boldsymbol{k} = (k,l)$. Using the correspondence $\partial_x \to \mathrm{i}k$ and $\partial_y \to \mathrm{i}l$, equation (3.15) and the incompressibility

condition (2.3) give

$$\mathrm{i}k\Big(U-\frac{\omega}{k}\Big)\hat{u}+\mathcal{D}U\ \hat{w}=-\mathrm{i}k\hat{p}+Re^{-1}\big(\mathcal{D}^2-|\boldsymbol{k}|^2\big)\hat{u}, \tag{3.17}$$

$$\mathrm{i}k\Big(U-\frac{\omega}{k}\Big)\hat{v}=-\mathrm{i}l\hat{p}+Re^{-1}\big(\mathcal{D}^2-|\boldsymbol{k}|^2\big)\hat{v}, \tag{3.18}$$

$$\mathrm{i}k\Big(U-\frac{\omega}{k}\Big)\hat{w}=-\mathcal{D}\hat{p}+Re^{-1}\big(\mathcal{D}^2-|\boldsymbol{k}|^2\big)\hat{w}, \tag{3.19}$$

$$\mathrm{i}k\hat{u}+il\hat{v}+\mathcal{D}\hat{w}=0. \tag{3.20}$$

The wavenumber vector $\boldsymbol{k}$ makes an angle θ with the direction $\hat{\boldsymbol{x}}$ of the background flow. Following Lin, we rotate the coordinate system by θ around the vertical axis directed by $\hat{\boldsymbol{z}}$. Note that it corresponds to a rotation of angle $-\theta$ for the vectors $\boldsymbol{x}$ and $\boldsymbol{u}$. We denote with a prime the variables in the new coordinate system. We stress that z, $\hat{w}(z)$ and $\hat{p}(z)$ are invariant under this rotation in the horizontal plane, and that the rotated background flow is no longer parallel:

$$\boldsymbol{U}'=\big(U(z)\cos(\theta),-U(z)\sin(\theta),0\big). \tag{3.21}$$

However, given that $k=|\boldsymbol{k}|\cos(\theta)$ and $l=|\boldsymbol{k}|\sin(\theta)$), we have

$$x'=x\cos(\theta)+y\sin(\theta)\qquad\Rightarrow\qquad|\boldsymbol{k}|x'=kx+ly. \tag{3.22}$$

Therefore, the perturbation characterized by equations (3.16*a*,*b*) no longer depends on the spanwise coordinate after rotation. Then, although the background flow is non-parallel, there is no need to use the general linearized equation (2.5). A straightforward way to obtain the counterpart of equations (3.17-3.20) in the new coordinate system is to write equation (3.15) in the prime variables[1] and then use the correspondence $\partial_{x'}\to\mathrm{i}|\boldsymbol{k}|$ and $\partial_{y'}\to 0$. This yields

$$\mathrm{i}|\boldsymbol{k}|\Big(U\cos(\theta)-\frac{\omega}{|\boldsymbol{k}|}\Big)\hat{u}\,'+\mathcal{D}U\ \cos(\theta)\hat{w}=-\mathrm{i}|\boldsymbol{k}|\hat{p}+Re^{-1}\big(\mathcal{D}^2-|\boldsymbol{k}|^2\big)\hat{u}\,', \tag{3.23}$$

$$\mathrm{i}|\boldsymbol{k}|\Big(U\cos(\theta)-\frac{\omega}{|\boldsymbol{k}|}\Big)\hat{v}\,'-\mathcal{D}U\ \sin(\theta)\hat{w}=Re^{-1}\big(\mathcal{D}^2-|\boldsymbol{k}|^2\big)\hat{v}\,', \tag{3.24}$$

$$\mathrm{i}|\boldsymbol{k}|\Big(U\cos(\theta)-\frac{\omega}{|\boldsymbol{k}|}\Big)\hat{w}=-\mathcal{D}\hat{p}+Re^{-1}\big(\mathcal{D}^2-|\boldsymbol{k}|^2\big)\hat{w}, \tag{3.25}$$

$$\mathrm{i}|\boldsymbol{k}|\hat{u}\,'+\mathcal{D}\hat{w}=0. \tag{3.26}$$

Next, we divide equations (3.23) and (3.25) by $\cos(\theta)$ and let

$$k'\equiv|\boldsymbol{k}|,\quad \omega'\equiv\frac{\omega}{\cos(\theta)},\quad Re'\equiv Re\cos(\theta)\quad\text{and}\quad\hat{p}\,'\equiv\frac{\hat{p}}{\cos(\theta)}. \tag{3.27}$$

[1] In particular, $U\to U\ \cos(\theta)$ and $\frac{d\boldsymbol{U}}{dz}\to\frac{d\boldsymbol{U}'}{dz}$.

In the new coordinate system, we end up with a closed set of equations for a two-dimensional perturbation:

$$\mathrm{i}k'\Big(U-\frac{\omega'}{k'}\Big)\hat{u}\,' + \mathcal{D}U\;\hat{w} = -\mathrm{i}k'\hat{p}\,' + Re'^{-1}\big(\mathcal{D}^2-k'^2\big)\hat{u}\,', \tag{3.28}$$

$$\mathrm{i}k'\Big(U-\frac{\omega'}{k'}\Big)\hat{w} = -\mathcal{D}\hat{p}\,' + Re'^{-1}\big(\mathcal{D}^2-k'^2\big)\hat{w}, \tag{3.29}$$

$$\mathrm{i}k'\hat{u}\,' + \mathcal{D}\hat{w} = 0. \tag{3.30}$$

Hence, we reduced the dimension of the perturbation, keeping only the component which propagates in the direction of the background flow. While doing so, we obtained a smaller Reynolds number, Re', and a larger growth rate, $\mathrm{Im}\{\omega'\}$. As we are interested in the most unstable perturbation, characterized by the minimum critical value of the Reynolds number and the highest growth rate, we can safely focus on two-dimensional perturbations in the remaining sections of this chapter.

3.4 Orr-Sommerfeld and Rayleigh equations

For a parallel shear flow, the background vorticity is $\boldsymbol{\Omega} = \Omega(z)\;\hat{\boldsymbol{y}}$ with $\Omega \equiv \mathcal{D}U$. Let ζ be the y-component of the perturbation vorticity, $\boldsymbol{\omega}$. The vorticity equation (2.9) becomes[1]

$$(\partial_t + U\partial_x)\zeta + w\frac{d\Omega}{dz} = Re^{-1}(\partial_x^2+\partial_z^2)\zeta. \tag{3.31}$$

As we have a two-dimensional incompressible flow, we conveniently introduce a streamfunction $\psi(x,z,t)$ such that

$$u = \partial_z\psi, \qquad w = -\partial_x\psi \qquad \text{and} \qquad \zeta = (\partial_x^2+\partial_z^2)\psi. \tag{3.32a,b,c}$$

Again, we seek normal modes in the form

$$\psi(x,z,t) = \mathrm{Re}\left\{\hat{\psi}(z)\;e^{\mathrm{i}k(x-ct)}\right\}, \tag{3.33}$$

where $c \equiv \omega/k$ is a complex phase speed. Then, equation (3.31) gives the so-called Orr-Sommerfeld equation:

$$(U-c)(\mathcal{D}^2-k^2)\hat{\psi} - \mathcal{D}^2U\;\hat{\psi} = (\mathrm{i}kRe)^{-1}[\mathcal{D}^2-k^2]^2\hat{\psi}. \tag{3.34}$$

In the inviscid limit, $Re\to\infty$, equation (3.34) becomes the Rayleigh equation:

$$(U-c)(\mathcal{D}^2-k^2)\hat{\psi} - \mathcal{D}^2U\;\hat{\psi} = 0. \tag{3.35}$$

We note that if $\hat{\psi}$ is solution of equation (3.35) for the eigenvalue c, then the complex conjugate, $\hat{\psi}^*$, is also solution for the eigenvalue c^*.

[1] In 2D, the vortex stretching terms vanish.

3.5 Solutions of the Rayleigh equation

In this section, we derive historical solutions the Rayleigh equation using standard techniques of analysis of ordinary differential equations (ODEs), an account of which can be found in Chapters 1 and 3 in the book by Bender and Orszag [34].

3.5.1 Heisenberg series

A set of solutions of the Rayleigh equation was first found in 1924 by Heisenberg [35], during his doctoral work with Sommerfeld. We give here a short derivation of his result.

Instead of the streamfunction, we can equivalently work with the displacement field of streamlines. The streamlines of the background flow are horizontal and are distorted by the perturbation. Let $\phi(x,z,t)$ be the displacement of a streamline which was located at height z in the base state. A kinematic condition requires the material derivative of that displacement to be equal to the vertical velocity, that is after linearization

$$(\partial_t + U\partial_x)\phi = -\partial_x \psi, \tag{3.36}$$

where we made a connection with the streamfunction using the relation (3.32*b*). For normal modes,

$$\phi(x,z,t) = \mathrm{Re}\left\{\hat{\phi}(z)\, e^{\mathrm{i}k(x-ct)}\right\}, \tag{3.37}$$

equation (3.36) yields

$$\hat{\phi} = -\frac{\hat{\psi}}{U-c}. \tag{3.38}$$

Then, from the Rayleigh equation (3.35) we readily obtain

$$\mathcal{D}^2\hat{\phi} + \frac{\mathcal{D}\hat{\phi}}{U-c} - k^2\hat{\phi} = 0. \tag{3.39}$$

The idea of Heisenberg was to look for solutions of equation (3.39) as series of the form

$$\hat{\phi} = \sum_{n=0}^{+\infty} \hat{\phi}_n k^{2n}. \tag{3.40}$$

On the one hand, the leading order term of the series evidently satisfies

$$\mathcal{D}^2\hat{\phi}_0 + \frac{\mathcal{D}\hat{\phi}_0}{U-c} = 0, \tag{3.41}$$

which can be regarded as a first order ODE for $\mathcal{D}\hat{\phi}_0$. After a straightforward integration, we find two linearly independent solutions:

$$\hat{\phi}_{0,1}(z) = 1 \qquad \text{and} \qquad \hat{\phi}_{0,2}(z) = \int^z \frac{d\tilde{z}}{[U(\tilde{z}) - c]^2}. \tag{3.42a,b}$$

On the other hand, we insert the ansatz (3.40) into equation (3.39) and obtain

$$\mathcal{D}^2\hat{\phi}_n + \frac{\mathcal{D}\hat{\phi}_n}{U-c} = k^2\hat{\phi}_{n-1} \qquad \text{for} \qquad n \geq 1. \tag{3.43}$$

Equation (3.43) is a first order linear inhomogeneous ODE for $\mathcal{D}\hat{\phi}_n$. Using the integrating factor $[U-c]^2$, we find the following recursion relation:

$$\hat{\phi}_n(z) = \int^z \frac{d\tilde{z}}{[U(\tilde{z}) - c]^2} \int^{\tilde{z}} d\zeta [U(\zeta) - c]^2 \hat{\phi}_{n-1}(\zeta). \tag{3.44}$$

Hence, the Heisenberg series are

$$\hat{\psi} = (U-c)\sum_{n=0}^{+\infty} \hat{\phi}_n k^{2n}, \tag{3.45}$$

where two possible $\hat{\phi}_0$ are given by (3.42*a,b*) and other terms of the series can be calculated using the recursion relation (3.44).

3.5.2 Tollmien inviscid solutions

Another set of solutions of the Rayleigh equation was found by Tollmien in 1929 [36], nowadays known as 'Tollmien inviscid solutions'. Before describing his approach, we recall the concept of singular point in ODEs.

Any second order linear homogeneous ODE can be written in the form

$$\mathcal{D}^2 f + p(z)\mathcal{D}f + q(z)f = 0. \tag{3.46}$$

By definition, z_c is a regular singular point if the coefficients $p(z)$ and $q(z)$ are not analytic at $z = z_c$ but there exists a neighborhood of z_c in the complex plane where $(z-z_c)p(z)$ and $(z-z_c)^2 q(z)$ are analytic. Any point where the coefficients $p(z)$ and $q(z)$ are analytic is an ordinary point. A point which is neither ordinary nor regular singular is an irregular singular point.

We write the Rayleigh equation (3.35) as

$$\mathcal{D}^2\hat{\psi} - \left(k^2 + \frac{\mathcal{D}^2 U}{U-c}\right)\hat{\psi} = 0, \tag{3.47}$$

and let z_c be a point in the complex plane such that

$$U(z_c) = c. \tag{3.48}$$

Because

$$\frac{\mathcal{D}^2 U}{U-c} \underset{z_c}{\sim} \frac{\mathcal{D}^2 U(z_c)}{\mathcal{D}U(z_c)(z-z_c)}, \tag{3.49}$$

z_c is a regular singular point. Following Tollmien, we seek solutions in the form of so-called Frobenius series:

$$\hat{\psi}(z) = \sum_{n=0}^{+\infty} a_j (z-z_c)^{j+\mathbb{s}}. \tag{3.50}$$

Inserting the ansatz (3.50) into equation (3.35) and expanding $U-c$ and $\mathcal{D}^2 U$ in Taylor series about $z = z_c$, we look for Frobenius exponents, $\mathbb{s}$, such that a solution for which $a_0 \neq 0$ exists. We find $\mathbb{s} = 0$ and $\mathbb{s} = 1$. As the difference between those values is an integer, we have two linearly independent solutions,

$$\hat{\psi}_1(z) = \sum_{n=0}^{+\infty} a_j (z-z_c)^{j+1}, \tag{3.51}$$

$$\text{and} \quad \hat{\psi}_2(z) = \sum_{n=0}^{+\infty} b_j (z-z_c)^{j} + C\ \hat{\psi}_1(z) \operatorname{Log}(z-z_c), \tag{3.52}$$

where Log is a complex extension of the natural logarithm. For $z < z_c$, Lin [33] justified that

$$\operatorname{Log}(z-z_c) = \begin{cases} \ln|z-z_c| - i\pi & \text{if} \quad \mathcal{D}U(z_c) > 0, \\ \ln|z-z_c| + i\pi & \text{if} \quad \mathcal{D}U(z_c) < 0. \end{cases} \tag{3.53}$$

According to Fuchs theorem, the radius of convergence of Frobenius series is equal to the distance from z_c to the nearest other singular point of the ODE (if any). We choose $a_0 = 1$ and $b_0 = 1$ and, to make sure that $\hat{\psi}_2$ does not contain any multiple of $\hat{\psi}_1$, we impose $b_1 = 0$. Next, elementary but heavy algebra gives

$$C = \frac{\mathcal{D}^2 U(z_c)}{\mathcal{D}U(z_c)} \tag{3.54}$$

and yields an infinitely countable set of relations from which the coefficients $a_1,\ a_2,\ a_3\ \ldots$ and $b_2,\ b_3,\ b_4\ \ldots$ can be recursively calculated. These coefficients are functions of k^2 and the derivatives of U at z_c.

3.5.3 Far field solutions

Using the transformation $z \to 1/z$, we can show that the Rayleigh equation has an irregular singular point at infinity. Hence, after Fuchs' theorem, the Tollmien inviscid solutions (3.51) and (3.52) are not valid at infinity. Similarly, the Heisenberg series (3.45) converge only a finite domain.

For background flows such that

$$\frac{\mathcal{D}^2 U}{U-c} \underset{z\to\pm\infty}{\longrightarrow} 0, \tag{3.55}$$

the Rayleigh equation (3.47) simplifies in the far field into

$$\mathcal{D}^2\hat{\psi} - k^2\hat{\psi} = 0. \tag{3.56}$$

Excluding divergent behaviors, we infer the following far field solutions:

$$\hat{\psi}(z) \underset{\pm\infty}{\sim} \mathcal{C}_\pm\, e^{\mp kz}, \tag{3.57}$$

where $\mathcal{C}_\pm$ are complex constants.

3.6 Inviscid results

In this section, we derive basic results on the stability of a parallel inviscid flow. The following relation, counterpart of equation (3.32*b*), will be useful;

$$\hat{w} = -\mathrm{i}k\hat{\psi}. \tag{3.58}$$

3.6.1 Pressure

In order to obtain an expression for the pressure amplitude, we eliminate $\hat{u}\,'$ in the horizontal momentum equation (3.28) using the incompressibility condition (3.30). Making use of relation (3.58) and removing the primes, we find[1]

$$\hat{p} = \hat{\psi}\mathcal{D}U - (U-c)\mathcal{D}\hat{\psi} \equiv \mathcal{W}(\hat{\psi}, U-c), \tag{3.59}$$

where $\mathcal{W}$ denotes the Wronskian of two functions. This is one of the very few cases where the pressure can be readily calculated from the velocity.

[1] We purposefully discarded the viscous term and we will keep doing so in the next subsections.

3.6.2 Wave-induced Reynolds stress

Inserting the components of the velocity vector (3.16*a*) for a normal mode into the definition of the Reynolds stress (3.7), we find

$$\tau_{\rm w}(z,t) = \hat{\tau}(z)\, e^{2k\,{\rm Im}\{c\}t} \qquad \text{where} \qquad \hat{\tau} \equiv -\frac{1}{2}\,{\rm Re}\{\hat{u}^*\hat{w}\}. \tag{3.60}$$

Relation (3.58) then gives an expression of the Reynolds stress amplitude in terms of the streamfunction,

$$\hat{\tau} = -\frac{k}{2}\,{\rm Im}\{\hat{\psi}\,\mathcal{D}\hat{\psi}^*\} = \frac{{\rm i}k}{2}\,\big(\hat{\psi}\,\mathcal{D}\hat{\psi}^* - \hat{\psi}^*\mathcal{D}\hat{\psi}\big) \equiv \frac{{\rm i}k}{2}\,\mathcal{W}(\hat{\psi},\hat{\psi}^*). \tag{3.61}$$

Hence, $\hat{\tau}$ is non-zero if, and only if, $\hat{\psi}$ and its complex conjugate, $\hat{\psi}^*$, are linearly independent. We now derive a key formula for the derivative of $\hat{\tau}$. According to the Leibniz rule,

$$\mathcal{D}\hat{\tau} = \frac{{\rm i}k}{2}\,\big(\hat{\psi}\,\mathcal{D}^2\hat{\psi}^* - \hat{\psi}^*\mathcal{D}^2\hat{\psi}\big). \tag{3.62}$$

We can extract $\mathcal{D}^2\hat{\psi}$ and $\mathcal{D}^2\hat{\psi}^*$ from the Rayleigh equation and its complex conjugate. After simple manipulations, we obtain

$$\mathcal{D}\hat{\tau} = \frac{{\rm i}k}{2}\,\mathcal{D}^2U\,|\hat{\psi}|^2\left(\frac{1}{U-c^*} - \frac{1}{U-c}\right) = k\,{\rm Im}\{c\}\,\frac{\mathcal{D}^2U\,|\hat{\psi}|^2}{2|U-c|^2}. \tag{3.63}$$

Equation (3.63) is the key ingredient in the derivations of the standard Rayleigh and Fjørtoft theorems, giving necessary conditions for a parallel inviscid flow to be unstable.

3.6.3 Necessary but not sufficient conditions of instability

• Rayleigh theorem from momentum conservation:

We start with the conservation of streamwise momentum (3.6) and use expression (3.60) for the Reynolds stress $\tau_{\rm w}(z,t)$. Invoking the result (3.63), we integrate between the horizontal boundaries, z_1 and z_2;

$$\partial_t\overline{\int_{z_1}^{z_2} dz\,u} = 0 = k\,{\rm Im}\{c\}\,e^{2k\,{\rm Im}\{c\}t}\int_{z_1}^{z_2} dz\,\frac{\mathcal{D}^2U}{2|U-c|^2}\,|\hat{\psi}|^2. \tag{3.64}$$

Hence, either ${\rm Im}\{c\} = 0$, that is the base state is neutrally stable, or the integral on the right-hand side of equation (3.64) vanishes. If ${\rm Im}\{c\} \neq 0$, then the vanishing of the integral implies that the background flow has an inflection point, that is there exists a height z_I at which $\mathcal{D}^2U(z_I) = 0$. This is the Rayleigh condition for the instability of a parallel inviscid flow.

• Fjørtoft theorem from energy conservation:

We start with the conservation of energy (3.14). We integrate by part using the boundary conditions (3.8*a*,*b*),

$$\partial_t \overline{\int_{z_1}^{z_2} dz\, K} = -\int_{z_1}^{z_2} dz\, U\, \frac{d\tau_{\rm w}}{dz}. \tag{3.65}$$

From the definition (3.11) of the kinetic energy, we find after some simple algebra that

$$\overline{K} = \frac{1}{4}\Big(|\mathcal{D}\hat{\psi}|^2 + k^2|\hat{\psi}|^2\Big)e^{2k\,\mathrm{Im}\{c\}t}. \tag{3.66}$$

We insert (3.66) into the left-hand side of (3.65) and invoke (3.63) on the right-hand side to obtain

$$\int_{z_1}^{z_2} dz\Big(|\mathcal{D}\hat{\psi}|^2 + k^2|\hat{\psi}|^2\Big) = -\int_{z_1}^{z_2} dz\, \frac{U\,\mathcal{D}^2 U}{|U-c|^2}\,|\hat{\psi}|^2. \tag{3.67}$$

If $\mathrm{Im}\{c\} \neq 0$, then we recall that the integral on the right-hand side of equation (3.64) is necessarily zero. We multiple this vanishing integral by $U(z_I) \equiv U_I$ and combine the result with the right-hand side of equation (3.67) to obtain

$$\int_{z_1}^{z_2} dz\, \frac{\mathcal{D}^2 U\,(U-U_I)}{|U-c|^2}\,|\hat{\psi}|^2 = -\int_{z_1}^{z_2} dz\Big(|\mathcal{D}\hat{\psi}|^2 + k^2|\hat{\psi}|^2\Big) < 0. \tag{3.68}$$

We infer the Fjørtoft condition for the instability of a parallel inviscid flow: $\mathcal{D}^2 U\,(U-U_I) < 0$ somewhere in the flow. Hence, energy conservation gives a stronger necessary condition of instability than momentum conservation but still not sufficient.

4. Interfacial waves

> *Il y a miracle si l'on accepte les explications surnaturelles. Il y a phénomène naturel si l'on recherche et si on trouve les causes physiques, capable de susciter le miracle apparent.*
>
> – **Maurice Leblanc**, L'Île aux trente cercueils, 1919.

In this chapter, we give some background on interfacial waves [37]. In section 4.1, we formulate the problem using the theory of potential flows and derive the linearized boundary conditions. Then, we show how to obtain the general dispersion relation of interfacial waves in section 4.2, before considering various limiting cases in section 4.3. All variables are dimensional.

4.1 Formulation of the problem

We consider a two-dimensional interface between two fluids of different densities. We canonically call the upper fluid air, with density ρ_a, and the lower fluid water, with density ρ_w. The air layer is semi-infinite while the water layer has a constant depth, h. There is no lateral boundary and we assume that both fluids are inviscid. The interface is planar, located at $z=0$, when the two fluids are at rest. An external perturbation sets up a displacement field, $\eta(x,y,t)$, and the interface becomes $z=\eta(x,y,t)$. A velocity field, $\boldsymbol{u}(\boldsymbol{x},t)$, is subsequently induced in both air and water. Because the densities are constant, the flow is incompressible, namely $\nabla\cdot\boldsymbol{u}=0$. Furthermore, it is irrotational[1] so we introduce a velocity potential, $\Phi(\boldsymbol{x},t)$, such that $\boldsymbol{u}=\nabla\Phi$. The incompressibility condition then yields the Laplace equation:

$$\nabla^2\Phi=0. \tag{4.1}$$

We need to establish the boundary conditions. At the interface, the vertical velocity must be continuous, equal to the material derivative of the displacement, that is

$$w=(\partial_t+\boldsymbol{u}\cdot\nabla)\eta \qquad \text{at} \qquad z=\eta^{\pm}. \tag{4.2}$$

Equation (4.2) is a kinematic boundary condition. The perturbation propagates due to two restoring forces: gravity, g, and surface tension, σ. Because of the

[1] After Lagrange's theorem, an inviscid flow remains irrotational if it was at $t=0$.

latter, the pressure is discontinuous at the interface, with a jump given by the Young-Laplace law:

$$p|_{z=\eta^+} - p|_{z=\eta^-} = \sigma \, \nabla \cdot \boldsymbol{n}_{\mathrm{a}\to\mathrm{w}}, \tag{4.3}$$

where

$$\boldsymbol{n}_{\mathrm{a}\to\mathrm{w}}(x,y,t) \equiv \frac{\nabla(\partial_x\eta, \partial_y\eta, -1)}{\sqrt{1+[\partial_x\eta]^2+[\partial_y\eta]^2}} \tag{4.4}$$

is a normal unit vector, oriented from air to water. Equation (4.3) is a dynamic boundary condition. A relation between the pressure and the velocity potential is given by Bernoulli's theorem, which states that

$$\partial_t\Phi + \frac{1}{2}|\nabla\Phi|^2 + gz + \frac{p}{\rho} = f(t), \tag{4.5}$$

where f is an arbitrary function. We choose $f = 0$ for convenience. In order to linearize the boundary conditions (4.2) and (4.3), we assume that the interface has a small slope. Formally, we let $\varepsilon \equiv \sqrt{|\partial_x\eta|^2 + |\partial_y\eta|^2} \ll 1$ and rescale the displacement field as $\eta \to \varepsilon\eta$. Proceeding as explained in the chapter 2, we collect terms of order ε. Then, equations (4.2) and (4.3) becomes

$$\partial_z\Phi = \partial_t\eta \qquad \text{at} \qquad z = 0^{\pm}, \tag{4.6}$$

$$\text{and} \qquad \rho_{\mathrm{w}}\partial_t\Phi\big|_{z=0^-} - \rho_{\mathrm{a}}\partial_t\Phi\big|_{z=0^+} + (\rho_{\mathrm{w}} - \rho_{\mathrm{a}})g\eta = \sigma(\partial_x^2 + \partial_y^2)\eta, \tag{4.7}$$

respectively. We need two more boundary conditions. Firstly, the air flow must be quiescent in the far field. Secondly, water cannot penetrate the rigid bottom boundary so the vertical velocity must vanish at $z = -h$. Hence, we have

$$\lim_{z\to+\infty} \Phi(x,y,z,t) = 0 \qquad \text{and} \qquad \partial_z\Phi|_{z=-h} = 0. \tag{4.8a,b}$$

In the next section, we solve the Laplace equation (4.1) with the boundary conditions (4.6), (4.7) and (4.8a,b).

4.2 Dispersion relation

Searching for normal modes, we assume a displacement field and a velocity potential of the form

$$\eta(x,y,t) = \mathrm{Re}\left\{\hat{\eta}\, e^{\mathrm{i}(kx+ly-\omega t)}\right\} \qquad \text{and} \qquad \Phi(x,z,t) = \mathrm{Re}\left\{\hat{\Phi}(z)\, e^{\mathrm{i}(kx+ly-\omega t)}\right\}, \tag{4.9a,b}$$

respectively. We insert (4.9b) into the Laplace equation (4.1) and obtain

$$\hat{\Phi}'' - (k^2+l^2)\hat{\Phi} = 0. \tag{4.10}$$

After imposing the boundary conditions (4.8*a*,*b*), we find

$$\hat{\Phi}(z) = \begin{cases} \Phi_\mathrm{a}\, e^{-|\boldsymbol{k}|z} & \text{if } z > 0, \\ \Phi_\mathrm{w}\, \cosh[|\boldsymbol{k}|(z+h)] & \text{otherwise,} \end{cases} \tag{4.11}$$

where Φ_a and Φ_w are complex constants, and $\boldsymbol{k} = (k,l)$ is a vector wavenumber defining the direction in which the wave propagates. The boundary conditions (4.6) and (4.7) at the interface yield

$$\begin{pmatrix} -\mathrm{i}\omega & |\boldsymbol{k}| & 0 \\ \mathrm{i}\omega & 0 & |\boldsymbol{k}|\sinh(|\boldsymbol{k}|h) \\ (\rho_\mathrm{w}-\rho_\mathrm{a})g+\sigma|\boldsymbol{k}|^2 & \mathrm{i}\omega\rho_\mathrm{a} & -\mathrm{i}\omega\rho_\mathrm{w}\cosh(|\boldsymbol{k}|h) \end{pmatrix} \begin{pmatrix} \hat{\eta} \\ \Phi_\mathrm{a} \\ \Phi_\mathrm{w} \end{pmatrix} = 0. \tag{4.12}$$

The vanishing of the determinant gives the dispersion relation

$$\omega^2 = \frac{(\rho_\mathrm{w}-\rho_\mathrm{a})g|\boldsymbol{k}| + \sigma|\boldsymbol{k}|^3}{\rho_\mathrm{a}+\rho_\mathrm{w}\operatorname{cotanh}(|\boldsymbol{k}|h)}. \tag{4.13}$$

Equation (4.13) has a positive and a negative root, corresponding to waves travelling forward and backwards in time, respectively. We consider only the positive root.

The right hand-side of equation (4.13) depends on the modulus of $\boldsymbol{k}$, not its components. Thus we orient the x-axis in the direction of $\boldsymbol{k}$ and perform the transformation $|\boldsymbol{k}| \to k$. Note that $k > 0$ with this orientation. Moreover, the dispersion properties no longer depend on y. Hence, we reduced the propagation of waves to one dimension. We introduce the phase speed,

$$c \equiv \frac{\omega}{k} \tag{4.14}$$

and rewrite equation (4.13) as

$$c^2 = \frac{1-r}{r+\operatorname{cotanh}(kh)}\left(1+\frac{1}{(1-r)Bo}\right)\frac{g}{k}, \tag{4.15}$$

where

$$r \equiv \frac{\rho_\mathrm{a}}{\rho_\mathrm{w}} \qquad \text{and} \qquad Bo \equiv \frac{\rho_\mathrm{w} g}{\sigma k^2} \tag{4.16a,b}$$

are the density ratio and the Bond number, respectively. The Bond number accounts for the competition between gravity and surface tension.

4.3 Wave zoology

We are interested in the dependence of the phase speed, c, on the wavenumber, k. Nonetheless, equation (4.15) also depends on three dimensionless numbers:

kh, r and Bo. It is difficult to extract any behavior when these numbers are all of order 1. However, we can simplify equation (4.15) by considering limits when some of them are very small or very large. This is a first example of asymptotic analysis.

4.3.1 Surface gravity waves

For the actual air-water interface, the density ratio is $r = O(10^{-3})$, thus we take $r = 0$ in equation (4.15). In so doing, we approximate interfacial waves with surface waves. Next, we assume that $Bo \gg 1$ that is we discard the effect of surface tension. We obtain

$$c = \sqrt{\tanh(kh)\frac{g}{k}}. \tag{4.17}$$

Equation (4.17) is the dispersion relation of (surface) gravity waves in **finite depth**, namely $kh = O(1)$. On the one hand, we consider waves with a wavelength $2\pi/k$ ranging from millimeter to hundreds of meters. On the other hand, the water depth, h, varies from decimeter to several kilometers. Hence, we can further simplify equation (4.17) by considering two limiting cases:

(i) Waves in **deep water**: $kh \gg 1$. Then $\tanh(kh) \sim 1$, and

$$c = \sqrt{\frac{g}{k}}. \tag{4.18}$$

(ii) Waves in **shallow water**: $kh \ll 1$. Then $\tanh(kh) \sim kh$, and

$$c = \sqrt{gh}. \tag{4.19}$$

Hence, the phase speed of gravity waves is independent of the wavenumber, k, in shallow water – that is there is no dispersion – while it has a power law behavior, $k^{-\frac{1}{2}}$, in deep water.

4.3.2 Effect of surface tension

In order to assess when it is valid to discard the effect of surface tension, we introduce the capillary wavenumber

$$k_{\text{cap}} \equiv \sqrt{\frac{\rho_{\text{w}} g}{\sigma}}, \tag{4.20}$$

and rewrite the Bond number as

$$Bo = \left[\frac{k_{\text{cap}}}{k}\right]^2. \tag{4.21}$$

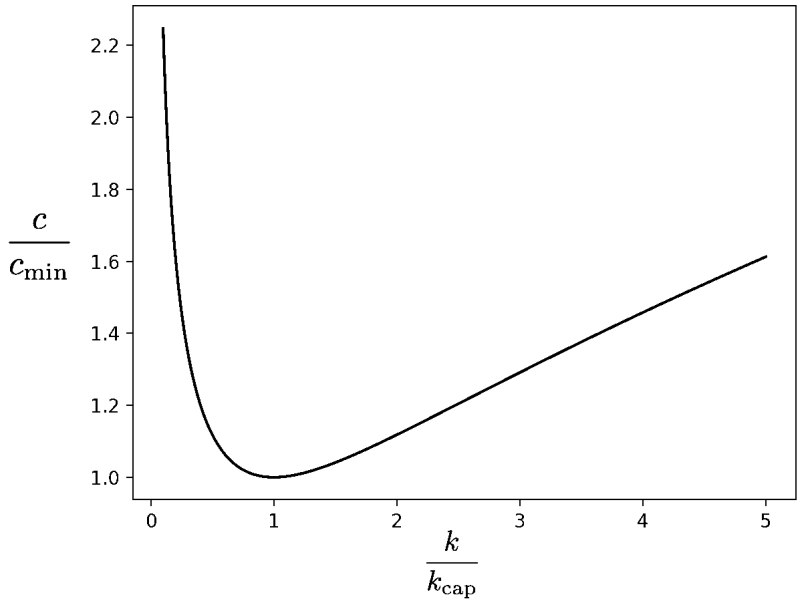

Figure 4.1: Dispersion relation of capillary-gravity waves.

Therefore, in subsection 4.3.1 we actually assumed that $k \ll k_{\text{cap}}$. For water, $k_{\text{cap}} = 370$ m^{-1} or, more intuitively, the capillary wavelength is $\lambda_{\text{cap}} \equiv 2\pi/k_{\text{cap}} = 17$ mm. Hence, the effect of surface tension is negligible for water waves whose wavelength is much larger than centimeter. Note that for $h > 10$ cm, we have $k_{\text{cap}}h \gg 1$ so that taking capillary effects into account implies to work in the deep water approximation, $kh \gg 1$. We distinguish two cases:

(i) **Capillary waves**: when $k \gg k_{\text{cap}}$, surface tension is the only restoring force and

$$c = \sqrt{\frac{\sigma k}{\rho_{\text{w}}}}. \tag{4.22}$$

(ii) **Capillary-gravity waves**: when $Bo = O(1)$, namely neither gravity nor surface tension dominates,

$$c = \sqrt{\frac{g}{k} + \frac{\sigma k}{\rho_{\text{w}}}}. \tag{4.23}$$

Hence, the square of the phase speed of capillary-gravity waves is equal to the sum of squares of the phase speeds of gravity waves and capillary

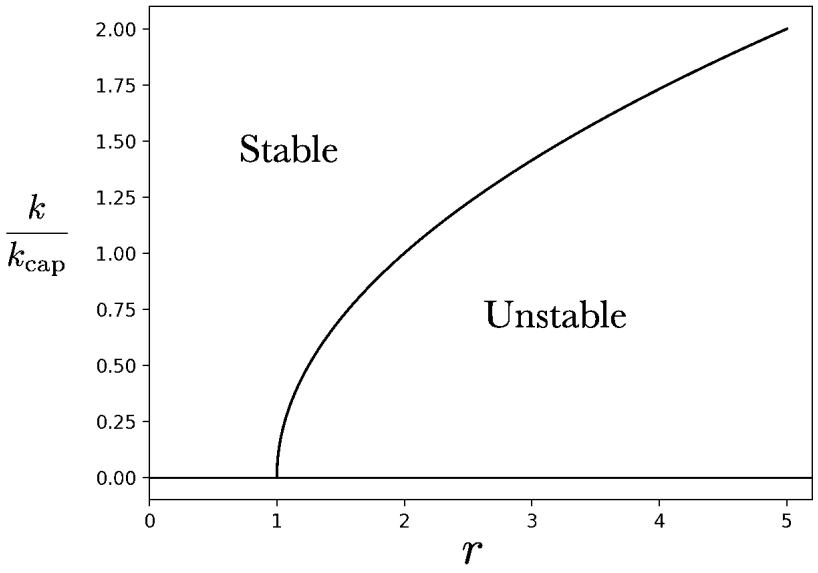

Figure 4.2: Curve of marginal stability for the Rayleigh-Taylor instability.

waves. The balance between the two restoring force leads to a minimum phase speed,

$$c_{\mathrm{min}} \equiv \left[\frac{4\sigma g}{\rho_{\mathrm{w}}}\right]^{\frac{1}{4}}, \tag{4.24}$$

reached at $k = k_{\mathrm{cap}}$; see Figure 4.1. Thus, we can write equation (4.23) as

$$c = \frac{c_{\mathrm{min}}}{\sqrt{2}}\sqrt{\frac{k_{\mathrm{cap}}}{k} + \frac{k}{k_{\mathrm{cap}}}}. \tag{4.25}$$

For water waves, $c_{\mathrm{min}} = 23$ cm.s^{-1}.

4.3.3 Interfacial waves in deep water and Rayleigh-Taylor instability

When the two fluids have close densities, it is no more valid to take $r = 0$. Then, the dispersion relation (4.23) of capillary-gravity waves becomes

$$c = \sqrt{At\,\frac{g}{k} + \frac{\sigma k}{\rho_{\mathrm{w}}(1+r)}}, \tag{4.26}$$

where

$$At \equiv \frac{1-r}{1+r} \tag{4.27}$$

is the Atwood number. Note that $c \in \mathbb{R}$ for all values of k when $At > 0$. In other words, confirming intuition, the interface between two fluids is neutrally stable when the lightest fluid lies above the heaviest. Any perturbation propagates at a phase speed given by equation (4.26). However, when $At < 0$, c is purely imaginary for $k < k_\star$, with

$$k_\star \equiv k_{\text{cap}}\sqrt{r-1}. \tag{4.28}$$

Thus, when a heavy fluid sits on the top of a lighter one, their interface is unstable to all perturbations having a wavenumber smaller than $k_\star$. This is a gravitational instability, studied by Lord Rayleigh and G. I. Taylor [38; 39]. Surface tension has a stabilizing effect: perturbations with a wavenumber larger than $k_\star$ become interfacial waves.

Regarding the density ratio, r, as a control parameter, equation (4.28) defines a curve of marginal stability (cf. chapter 2) plotted in Figure 4.2. In an experiment where r increases continuously, the critical density ratio is $r_c = 1$ and the critical wavenumber is $k_c = 0$.

4.3.4 From interfacial to surface waves

Let c_{int} and c_{surf} be the phase speeds of interfacial and surface waves, given by equations (4.26) and (4.23) respectively. Simple algebra gives

$$\frac{c_{\text{int}}}{c_{\text{surf}}} = \sqrt{\frac{1}{1+r} - \frac{r}{1+\left[\frac{k}{k_{\text{cap}}}\right]^2}}. \tag{4.29}$$

The density ratio, r, is a measure of the coupling between the two fluid layers. For $r \ll 1$, the relative change of the phase speed of surface waves due to that coupling is

$$\frac{c_{\text{int}} - c_{\text{surf}}}{c_{\text{surf}}} = -\frac{r}{2}\left(1 + \frac{1}{1+\left[\frac{k}{k_{\text{cap}}}\right]^2}\right) + \mathcal{O}\left(r^2\right). \tag{4.30}$$

Hence, an interfacial wave is slower than a surface wave.

5. Wind, waves, current and asymptotic analysis

C'est pas l'homme qui prend la mer, c'est la mer qui prend l'homme.
Moi, la mer, elle m'a pris, au dépourvu, tant pis!
– **Renaud**, Dès que le vent soufflera, 1983.

In this chapter, we summarize our work on the interaction of interfacial waves with a parallel shear flow. We formulate in section 5.1 a general eigenvalue problem for flow driven interfacial waves. In section 5.2, we review the Miles theory of wind-waves, which is based on two key assumptions: the air-water density ratio is a small parameter and there is no background flow in the water. We describe our numerical scheme to solve the Rayleigh equation in section 5.3 and our asymptotic analysis of wind-waves in section 5.4. Finally, we relax the assumptions of Miles in section 5.5 and present our results on instabilities of flow driven interfacial waves. All variables are dimensional.

5.1 Eigenvalue problem for flow driven interfacial waves

We consider interfacial waves in presence of a parallel shear flow, $U(z)$, depicted in Figure 5.1. We call 'wind' the flow in air and 'current' the flow in water. How does this flow affect the dispersion relation of the waves? The shear brings vorticity so the potential theory used in chapter 4 no longer applies. Instead, we formulate the problem in the framework of hydrodynamic stability, introduced in chapters 2 and 3. Hence, we regard the waves as perturbations of the parallel flow. For simplicity, we work in the deep water limit – equivalent to infinite depth – and consider only two-dimensional perturbations, assuming that the Squire theorem holds[1]. So the perturbed flow is completely described by a streamfunction, $\psi(x,z,t)$. In this linear treatment, the density remains a step function even in the presence of waves;

$$\rho(z) \equiv \begin{cases} \rho_{\mathrm{a}} & \text{if} \quad z > 0, \\ \rho_{\mathrm{w}} & \text{if} \quad z < 0. \end{cases} \tag{5.1}$$

[1] We check it a posteriori in PAPER I.

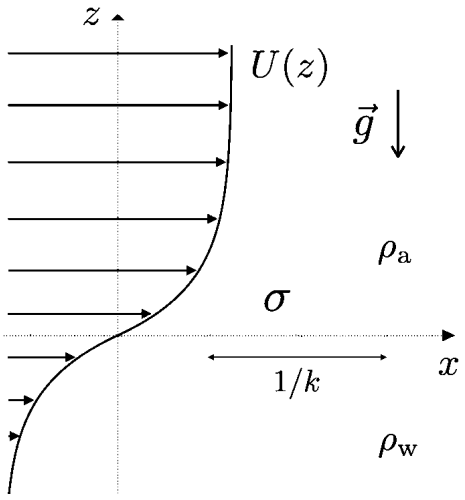

Figure 5.1: Schematic of interfacial waves in the presence of parallel shear flow.

We focus on the normal modes of the interface. According to section 3.4, the complex amplitude of the streamfunction, $\hat{\psi}(z)$, obeys the Rayleigh equation:

$$(U-c)(\hat{\psi}''-k^2\hat{\psi})-U''\hat{\psi}=0, \tag{5.2}$$

where prime now denotes the derivative with respect to z. We shall solve equation (5.2) in both air and water, and need boundary conditions at the interface. In section 3.5.1, we introduced the streamline displacement field, $\phi(x,z,t)$. Since the perturbed interface must be a streamline, the surface displacement field, $\eta(x,t)$, is given by

$$\eta(x,t)=\phi(x,z=0,t). \tag{5.3}$$

Therefore, the general kinematic condition for normal modes (3.38) gives at the interface

$$\hat{\eta}=-\frac{\hat{\psi}}{U-c}\bigg|_{z=0}. \tag{5.4}$$

As explained in section 4.1, the dynamic boundary condition is given by the pressure jump caused by surface tension. Here, it takes the form

$$[\hat{p}-\rho g\hat{\eta}]_{0^-}^{0^+}=-\sigma k^2\hat{\eta}, \tag{5.5}$$

where ρ is given by equation (5.1) and $\hat{p}(z)$ is the complex amplitude of the perturbation pressure of a normal mode. The latter is connected to the stream-

function amplitude, $\hat{\psi}(z)$, via equation (3.59) which we recall below for convenience[1];

$$\hat{p} = \rho\{\hat{\psi}U' - (U-c)\hat{\psi}'\}. \tag{5.6}$$

We stress that $\hat{\psi}$ is continuous at $z=0$ so long as U is itself continuous at $z=0$, as can be seen from equation (5.4). However, the derivatives U' and $\hat{\psi}'$ are discontinuous at $z=0$. We combine equations (5.4), (5.5) and (5.6) into

$$(\rho_w - \rho_a)g + \sigma k^2 + \rho_a \Xi(0^+) - \rho_w \Xi(0^-) = 0, \tag{5.7}$$

where we let

$$\Xi \equiv [c-U]^2 \frac{\hat{\psi}'}{\hat{\psi}} + U'(c-U). \tag{5.8}$$

The far field behavior of the solution of the Rayleigh equation was studied in section 3.5.3. Here, we impose that

$$\hat{\psi}' \pm k\hat{\psi} \underset{z\to\pm\infty}{\longrightarrow} 0. \tag{5.9}$$

We have formulated an eigenvalue problem for a sheared two-fluid interface, where the eigenvalue is the complex phase speed, c, and the eigenfunction is the streamfunction amplitude, $\hat{\psi}(z)$. For simplicity, we consider a wind-induced current so that the velocity of the background flow decays in water; see Figure 5.1.

5.2 Miles theory of wind-waves

Miles [13] noticed that wind and waves are weakly coupled because the air-water density ratio, $r = \rho_a/\rho_w$, is small. Hence, he proposed to expand the eigenvalue and eigenfunction in series of power of r;

$$c = c_0 + r\, c_1 + \ldots \qquad \text{and} \qquad \hat{\psi} = \hat{\psi}_0 + r\, \hat{\psi}_1 + \ldots, \qquad r \ll 1. \tag{5.10}$$

At the leading order, namely $r=0$, we have

$$(U-c_0)(\hat{\psi}_0'' - k^2\hat{\psi}_0) - U''\hat{\psi}_0 = 0, \tag{5.11}$$

$$\text{and} \quad g + \frac{\sigma}{\rho_w}k^2 - \left\{[c_0-U]^2\frac{\hat{\psi}_0'}{\hat{\psi}_0} + U'(c_0-U)\right\}_{z=0^-} = 0. \tag{5.12}$$

Here, c_0 is the phase speed of sheared surface waves, determined by the perturbed flow which they induce in water. That flow is itself described by $\hat{\psi}_0(z<$

[1]Density does not appear in equation (3.59) because a pressure scale $\rho^* V^{*2}$ was used to make it dimensionless.

0). The physical meaning of $\hat{\psi}_0(z>0)$ is more subtle. When we take $r=0$, we are not taking $U(z>0)$ to zero so we actually remove the air but keep the wind. It means that the waves do not see the wind (because there is no air) whereas the wind can still see the waves. Hence, $\hat{\psi}_0(z>0)$ describes the perturbation induced by waves on the wind without feedback (unlike in water). In other words, there is an intrinsic coupling between the current and the waves because water is the medium where they propagate, whereas r is the coupling constant between wind and waves. Wind-wave growth is expected at the next order of perturbation in r.

In order to decouple c_0 from $\hat{\psi}_0$, Miles made a further assumption: he discarded the current and thus took $U(z\leq 0)=0$. Then, the solution of the Rayleigh equation in the water is

$$\hat{\psi}_0(z\leq 0)=\hat{\psi}_0(0)e^{kz}. \tag{5.13}$$

Next, we insert $\hat{\psi}_0'(0^-)$ into equation (5.12), which becomes

$$g+\frac{\sigma}{\rho_{\mathrm{w}}}k^2-kc_0^2=0. \tag{5.14}$$

We conclude that, in the absence of current, c_0 is the phase speed of free surface waves in deep water (cf. Eq. 4.23). The value of c_0 being now known, we can solve – at least formally – the leading order Rayleigh equation (5.11) in the air. This is a simple boundary value problem where we can impose any non-zero value of $\hat{\psi}_0$ at $z=0$. Indeed, a linear theory does not determine the wave amplitude. The eigenvalue at the next order is

$$c_1=\frac{c_0}{2k}\frac{\hat{\psi}_0'(0^+)}{\hat{\psi}_0(0)}+\frac{U'(0^+)}{2k}-\frac{c_0}{2}\frac{1}{1+\left[\frac{k}{k_{\mathrm{cap}}}\right]^2}. \tag{5.15}$$

The last term in equation (5.15) comes from the difference between the phase speed of interfacial and surface waves (cf. section 4.3.4). Physical intuition leads us to expect a resonance at the critical level z_c such that

$$U(z_c)=c_0. \tag{5.16}$$

We expect an energy transfer from the background flow to the perturbation (from wind to waves) at the height where the phase speed of free surface waves equals the wind speed. This intuition was highlighted by Lighthill [14]. However, Miles [13] had already built up on the mathematical treatment of neutral modes by Lin [33] and shown that

$$\mathrm{Im}\left\{\frac{2c}{c_0}\right\}=-r\frac{\pi}{k}\frac{U''(z_c)}{|U'(z_c)|}\left|\frac{\hat{\psi}_0(z_c)}{\hat{\psi}_0(0)}\right|^2\equiv\gamma. \tag{5.17}$$

The left-hand side of equation (5.17) is the energy growth rate[1] normalized by the angular frequency of free surface waves. The right-hand side confirms that the energy transfer occurs at $z = z_c$ and is proportional to the coupling constant, r. Furthermore, a necessary condition for growth is a wind profile having a negative curvature. Although the energy transfer is localized at the critical level, we stress that it is a global problem: the local transfer is actually determined by the boundary condition at the water surface. In his seminal paper [13], Miles indeed used the following global property of the Rayleigh equation:

$$\mathrm{Im}\left\{\frac{\hat{\psi}_0'(0^+)}{\hat{\psi}_0(0)}\right\} = -\pi\frac{U''(z_c)}{|U'(z_c)|}\left|\frac{\hat{\psi}_0(z_c)}{\hat{\psi}_0(0)}\right|^2. \tag{5.18}$$

Equation (5.18) is the mathematical bridge between the eigenvalue at order r given by equation (5.15) and the Miles formula (5.17). Janssen [1] proposed a more physical derivation of the latter, based on the wave-induced Reynolds stress.

5.3 Numerical solution of the Rayleigh equation

The key result of Miles' theory is the formula (5.17) for the normalized growth rate, γ. In order to evaluate the latter for a given wind profile, $U(z)$, we need to solve the leading order Rayleigh equation (5.11) in the domain $[0, +\infty)$. We impose $\hat{\psi}_0(z = 0) = 1$ and a far field behavior given by equation (5.9). There is a regular singular point at $z = z_c$ which makes the resolution of this boundary-value problem challenging. It was solved numerically for the first time in 1959 by Conte and Miles [40], who designed a scheme specific to a logarithmic wind profile,

$$U(z) = u_\star \ln(1 + z/z_0)/\kappa, \tag{5.19}$$

where $u_\star$ is the friction velocity associated with a constant shear stress, z_0 is the roughness length accounting for the presence of waves on the water surface and $\kappa \simeq 0.4$ is the von Kármán constant. The log profile (5.19) comes from the theory of turbulent boundary layers [41] and has been supported by experiments [16] and direct numerical simulations [17].

In 1965, Hughes and Reid [42] described a general numerical scheme to solve the Rayleigh equation and provided meanwhile an exact analytical solution for an exponential profile,

$$U(z) = U_0\left(1 - e^{-z/d}\right), \tag{5.20}$$

[1] It is twice the growth rate of wave amplitude.

also known as the asymptotic suction profile. In equation (5.20), U_0 is the far-field velocity and d is the thickness of the suction layer. Hughes and Reid were interested in the general stability of parallel flows rather than in the wind-wave problem. About forty years later, Beji and Nadaoka [43] computed the normalized growth rate, γ, for various wind profiles. They used a variant of Hughes and Reid's method, whose paper they nonetheless did not cite. Our own scheme to solve the leading order Rayleigh equation (5.11) is inspired by these earlier work. We use the Tollmien inviscid solutions (3.51) and (3.52) to define a local solution around the singularity at $z = z_c$;

$$\hat{\psi}_{\text{loc}}(z) \equiv A(z - z_c) + B\left\{1 + \frac{U''(z_c)}{U'(z_c)}(z - z_c)\,\text{Log}(z - z_c)\right\}, \tag{5.21}$$

where A and B are complex constants to be determined. The complex logarithm was defined in equation (3.53). As we only need a local solution, it is sufficient to keep only the first terms in the Frobenius series. We separate the real and imaginary parts of equation (5.21) and integrate each numerically from $z_c - \delta$ to $z = 0$, and from $z_c + \delta$ to z_∞, with a jump $\delta = O(10^{-6})$. The upper boundary of integration, z_∞, is such that

$$e^{-kz_\infty} = O(10^{-3}). \tag{5.22}$$

While the complex coefficients A and B are still unknown, we enforce the boundary condition (5.9) at $z = z_\infty$ and require $\hat{\psi}_0(z = 0) = 1$. This yields a linear fourth-order system for the real and imaginary parts of A and B, which we solve analytically. We stress that $\hat{\psi}_0(z_c) = B$ and thus directly evaluate Miles' formula (5.17) for the normalized growth rate. We can further integrate upward and downward the local solution (5.21) with the known values of A and B, and infer the perturbation streamfunction at any point of the flow.

Let us note Morland and Saffman [44] solved the full eigenvalue problem numerically and demonstrated the accuracy of Miles theory for $r = O(10^{-3})$.

5.4 Wind-wave asymptotics

In an Appendix of Morland and Saffman's paper [44], Miles used the exact analytical solution of the Rayleigh equation for the exponential profile (5.20) to calculate γ. However, the result involves hypergeometric functions. In order to obtain an explicit behavior of γ as a function of the wavenumber, k, Miles performed an asymptotic analysis of γ for long and short waves that is $kd \ll 1$ and $kd \gg 1$, respectively. Since an exact solution of the Rayleigh equation is in general out of reach – especially for the log profile (5.19) – we propose to perform an asymptotic analysis directly on the Rayleigh equation.

5.4.1 Long wave analysis

We want to solve the leading order Rayleigh equation (5.11) for the log profile (5.19) and use the solution to calculate the normalized growth rate, γ, via the Miles formula (5.17). On the one hand, according to experimental data, the roughness length, z_0, is of order of a millimeter. On the other hand, we are interested in capillary-gravity waves with wavelengths ranging from a few millimeters to hundreds of meters. From this scale separation, we construct a small parameter

$$kz_0 \ll 1. \tag{5.23}$$

In this chapter, we have so far worked with dimensional variables. We now make all variables dimensionless using the roughness length, z_0, and the friction velocity, $u_\star$. **We denote dimensionless variables with the same symbol as their dimensional counterpart.** In particular, we now have $k \ll 1$ after equation (5.23). We use this small parameter to find asymptotic solutions of the leading order Rayleigh equation, written in the form

$$\hat{\psi}_0'' - \left(k^2 + \frac{U''}{U - c_0}\right)\hat{\psi}_0 = 0, \qquad k \ll 1. \tag{5.24}$$

In section 3.5, we derived the series solutions found by Heisenberg and stressed that they converge only on a finite domain. We also found the far field behavior of the solution of the Rayleigh equation. Here, we connect these two pieces of solution using the small parameter $k \ll 1$ in a procedure called asymptotic matching. It was inspired by Examples 2, 3 and 4 from Chapter 7 in the book by Bender and Orszag [34]. We can show that the Heisenberg series are valid solutions at the water surface, $z = 0$, and at the critical layer, $z = z_c$. The key is to find the height z_s where those series become invalid and have to be replaced by the far field solution.

The log profile satisfies Miles' necessary condition for wave growth and has a negative curvature, namely $U'' < 0$, and we evidently have $U > c_0$ for $z > z_c$. Hence, there exists a point z_s where the bracket in equation (5.24) vanishes, that is

$$k^2 + \frac{U''(z_s)}{U(z_s) - c_0} = 0. \tag{5.25}$$

We call outer region the interval $[0, z_s]$, where we define an outer solution from the first terms ($k = 0$) of the Heisenberg series:

$$\hat{\psi}_{\text{out}}(z) \equiv E\,(U(z) - c_0) + F\,(U(z) - c_0)\int^z \frac{d\tilde{z}}{[U(\tilde{z}) - c_0]^2}. \tag{5.26}$$

For $z > z_s$, we have the far field solution

$$\hat{\psi}_\infty(z) \equiv G\,e^{-kz}. \tag{5.27}$$

The complex constants E, F and G are determined by matching $\hat{\psi}_{\text{out}}$ and $\hat{\psi}_{\infty}$ as k goes to zero. We emphasize that z_s is a function of k and

$$\lim_{k\to 0} z_s(k) = +\infty \qquad \text{but} \qquad \lim_{k\to 0} k z_s(k) = 0. \tag{5.28}$$

Technical details and a comparison with the numerical solution of the Rayleigh equation can be found in PAPER I, as well as an explicit expression of γ as a function of k. In particular, we show that long waves interact with the wind all the way from the water surface to the critical level.

5.4.2 Strong wind limit

In this sub-section, we keep using dimensionless variables.

The long wave analysis provides an explicit dependence of the normalized growth rate, γ, as a function of the wavenumber, k. This dependence is however too complicated to extract the position, $k_{\max}$, and amplitude, $\gamma_{\max}$, of the maximum growth rate. For gravity waves, there is one control parameter: the Froude number, defined as

$$Fr \equiv \frac{u_\star}{\sqrt{g z_0}}, \tag{5.29}$$

and expressing the competition between the shear and the restoring force. We can simplify the function $\gamma(k)$ by taking the limit of large Froude number, or strong wind limit. Because it is more convenient to work with small rather than large parameters, we follow Young and Wolfe [18] and introduce

$$m \equiv Fr^{-2}. \tag{5.30}$$

Young and Wolfe took the limit $m \to 0$ on the function $\gamma(k)$ they had obtained from the exact analytical solution of the Rayleigh equation for the exponential profile (5.20). In PAPER I, we generalize the definition of m to capillary and capillary-gravity waves, and take the limit $m \to 0$ on various functions $\gamma(k)$ obtained from the long wave asymptotics. In particular, for the log profile we find that

$$k_{\max} \sim Fr^{-1} \qquad \text{and} \qquad \gamma_{\max} \sim Fr^2, \qquad Fr \gg 1. \tag{5.31}$$

This is a mathematical answer to the question 'what is the fastest growing wave?'. For a physical answer, we need to go back to the original motivation of Miles, who was actually inspired by the old work of Jeffreys [28].

5.4.3 On the aerodynamic pressure

In this sub-section, we go back to dimensional variables.

In 1925, Jeffreys [28] suggested that wind-waves grow provided that the aerodynamic pressure[1] is in phase with the wave slope, namely

$$p(x, z=0, t) \propto \partial_x \eta. \tag{5.32}$$

The proportionality constant was called the sheltering coefficient and had to be determined experimentally. Equation (5.32), known as the sheltering hypothesis, says that waves grow because the pressure on the windward side of a wave crest is greater than on the leeward side. The aim of Miles' theory was actually to provide a rational for this pressure asymmetry. The pressure amplitude of a normal mode, $\hat{p}(z)$, is given by equation (5.6), and the kinematic boundary condition (5.4) connects the streamfunction amplitude at $z = 0$ to the amplitude $\hat{\eta}$ of the surface displacement. Therefore, the aerodynamic pressure of a normal mode, $\hat{p}(z=0)$, is necessary proportional to $\hat{\eta}$. We justify in PAPER I that, for mathematical consistency, all physical quantities should be expanded in power of the density ratio, r; the leading order quantities are denoted with the index 0. Hence, we let γ and μ such that

$$\hat{p}_0(z=0) \equiv \rho_w c_0^2 (\mu + \mathrm{i}\gamma) k \hat{\eta}_0. \tag{5.33}$$

We show in PAPER I that the coefficient γ in equation (5.33) is the normalized growth rate given by the Miles formula (5.17). Moreover, μ is twice the wind-dependent relative change of the phase speed of water waves due to the coupling with the air. Our key result is that, in the strong wind limit, the maximum of γ occurs when μ vanishes. In other words, the fastest growing wave is such that the aerodynamic pressure is proportional to the wave slope. Hence, we provided the rational for Jeffreys' sheltering hypothesis which Miles was looking for.

5.5 Beyond Miles theory

We relax the two key assumptions of Miles on the eigenvalue problem for flow driven interfacial waves: we consider a density ratio r which is not necessarily small and account for the presence of a current in water. Young and Wolfe [18] found exact analytical solutions to the full eigenvalue problem for a double exponential profile, and provided physical intuition on the possible instabilities in this system. We write the complex phase speed as

$$c = U_S + \hat{c}_r + \mathrm{i}\, c_\mathrm{i}, \tag{5.34}$$

where $U_s \equiv U(z=0)$ is the surface drift, c_i is the imaginary of c and $\hat{c}_r$ is the intrinsic phase speed, that is the real part of c in the frame of the water surface. From equation (5.34), we define two types of modes:

[1] The aerodynamic pressure is the pressure set up by the wind above the waves.

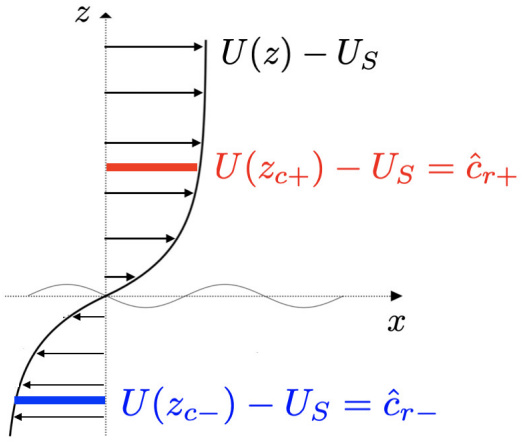

Figure 5.2: Schematic of the background flow and waves in the frame of the water surface, moving at the drift velocity, U_S. Prograde and retrograde modes have a critical layer in air and water, respectively.

1. A prograde mode has a positive intrinsic phase speed, $\hat{c}_{r+} > 0$.

2. A retrograde mode has a negative intrinsic phase speed, $\hat{c}_{r-} < 0$.

In other words, a mode is prograde if the actual phase speed of the sheared waves, $\mathrm{Re}\{c\}$, is greater than the surface drift; otherwise, it is retrograde. In the case of wind-induced current depicted in Figure 5.2, prograde and retrograde modes have critical layers at heights $z_{c+} > 0$ and $z_{c-} < 0$ such that

$$U(z_{c\pm}) - U_S = \hat{c}_{r\pm}. \tag{5.35}$$

Therefore, a prograde mode undergoes a Miles instability due to a critical layer in air whose location is unknown because of the intrinsic coupling with the current and the strong coupling with the wind (as r is not small). Analogously, a retrograde mode undergoes another instability, coined 'rippling instability' by Young and Wolfe [18], due to a critical layer in water whose location is unknown for the same reasons.

We find general asymptotic solutions of this eigenvalue problem using the small parameter

$$1/(kL_{\mathrm{w}}) \ll 1, \tag{5.36}$$

where L_{w} is a characteristic length scale of the current. We show that, in the limit of short wavelength, the two critical layers become internal boundary layers with thickness of order $1/k$. In an astrophysical context, Alexakis et al. [45] had proposed a solution based on the WKB method but we show that

their approach is incorrect. We obtain an asymptotic series for $\hat{c}_{r\pm}$, and calculate the growth rate $k\, c_{\mathrm{i}\pm}$ of the Miles and rippling instabilities using so-called exponential asymptotics. Details can be found in PAPER II.

6. Summary and outlook

There are more things in heaven and earth than are dreamt of in your philosophy.

– **Iron Maiden**, Dance of Death, 2003.

Motivated by the importance of ocean waves in the climate system as well as the appealing beauty of their mathematical modeling, we have studied the growth and propagation of waves in the presence of wind and current.

Firstly, we combined background knowledge in hydrodynamic stability and water waves to make a clear formulation of the Miles theory of wind-wave interaction. Assuming an infinitesimal amplitude, we linearized the Navier-Stokes equation. Next, the normal modes analysis for the stability of a parallel shear flow led to the Orr-Sommerfeld equation. Following Miles, we discarded the effect of viscosity by taking the Reynolds number to infinity, which gave the Rayleigh equation. Enforcing boundary conditions at the air-water interface, we obtained an eigenvalue problem for the complex phase speed and complex amplitude of the streamfunction. On the one hand, we simplified the eigenvalue problem using an expansion in power of the small air-water density ratio. The first order eigenvalue is obtained from the zeroth order eigenvalue and eigenfunction. On the other hand, we drew a connection between the eigenvalue and the pressure-displacement relation in the Fourier space. Waves grow because their interaction with the wind, while affecting their phase speed, induces a phase-shift between the aerodynamic pressure and the surface displacement. The density ratio – small parameter of the perturbative expansion – can be viewed as the coupling constant of that interaction. To the leading order, wind-waves are neutral modes and have a critical layer where the wind speed equals the phase speed of free surface waves. As a consequence, there is a non-zero wave-induced Reynolds stress, whose work on the water surface leads to a growth at the next order of perturbation.

Secondly, we solved the leading order Rayleigh equation, which has a regular singularity at the critical level. To do so, we noticed that most waves have a wavelength much larger than the characteristic length scale of the wind profile. Thus, we used the wavenumber as a small parameter and obtained approximate solutions by asymptotic matching. We inferred formulae for the growth rate of the Miles instability and the wind correction to the phase speed of free surface

waves. We simplified those formulae in the strong wind limit and realized that the growth rate is maximum when the wind correction to the phase speed vanishes. Equivalently, the condition of optimum growth is a phase shift equals to $\pi/2$, which corresponds to the aerodynamic pressure being in phase with the wave slope. This result was intuited by Jeffreys about a century ago. Hence, we needed five levels of asymptotics to confirm Jeffreys' intuition and finally answer the basic question 'what is the fastest growing wave?'. For clarity, we summarize these levels below:

1. $k\hat{\eta} \ll 1$: a small wave slope allows to linearize the Navier-Stokes equation.

2. $Re \to +\infty$: an infinite Reynolds number makes the effect of viscosity negligible; this limit determines the branch cut associated with the singularity of the Rayleigh equation [33].

3. $r \ll 1$: the small air-water density ratio, which corresponds to a weak coupling between wind and waves, helps to simplify the eigenvalue problem; in PAPER I, r was denoted ε.

4. $kz_0 \ll 1$: the scale separation between the wavelength of capillary-gravity waves and the roughness length of the logarithmic wind profile is the key to find asymptotic solutions of the Rayleigh equation.

5. $m \ll 1$: the control parameter m defined in PAPER I expresses the competition between the shear and the restoring forces; its smallness corresponds to the strong wind limit.

Thirdly, we went two steps further: we added a current in water and relaxed the Miles assumption of a small density ratio. We solved the corresponding eigenvalue problem using the dimensionless inverse wavenumber as a small parameter. In other words, we considered waves whose wavelength is much smaller than the characteristic length scales of the wind and current profiles. We assumed that the imaginary part of the phase speed was small and sought solutions of the Rayleigh equation with a real, still unknown, phase speed. Internal boundary layers emerge at the critical levels where the flow speed equals that unknown phase speed. For monotonic profiles, there is one boundary layer in air, and another in water. We looked for inner solutions valid around the critical levels and matched them with outer solutions, before constructing a uniformly valid composite solution. We stress that we did not need to specify the wind and current profiles explicitly. Next, we used that solution to find the explicit dependence of the boundary condition on the complex phase speed. We expanded the real part in a power series of the small parameter but had to

include transcendentally small terms to have a non-zero imaginary part. Our final expressions depend only on derivatives of the profile at the air-water interface and at the critical levels. Physically, it means that the interaction between the waves and the mean flow is localized in the internal boundary layers of thickness equal to the inverse of the wavenumber. The one in air is responsible for the Miles instability while the one in water is responsible for the rippling instability.

Perspectives

(i) Whereas the short wave expansions happened to be mathematically more powerful than the long wave asymptotics, they had narrower oceanographic applications. Indeed, most ocean waves are long and those which could be classified as short have a tiny growth rate for both the Miles and rippling instabilities. But given how fruitful the long wave analysis of wind-wave interaction was, it is very desirable to try and extend it to wave-current interaction. In particular, the location and amplitude of the maximum growth rate of the rippling instability is still unknown.

(ii) There is very few work going beyond the linear theory of wind-wave interaction. On the one hand, Janssen [46] derived in 1982 a quasi-linear model that includes the effect of the growing waves on the wind profile. In other words, the growth rate of the Miles instability became time-dependent. Janssen obtained a non-linear diffusion equation for the wind velocity, to be solved simultaneously with the Rayleigh equation and the evolution equation for the wavenumber spectrum. The solution of this system of equations has been overlooked in the literature, principally because of the singular structure of the Rayleigh equation. On the other hand, Zdyrski and Feddersen [47] recently investigated the effect of wind on Stokes waves in deep water using a parametric pressure forcing inspired by the Miles mechanism. They included weak non-linear effects in the water, as Stokes waves have a dispersion relation depending on the wave amplitude. However, their coupling with air was not dynamical because the pressure above the waves was parametrized instead of being calculated. We propose to combine the Janssen model [46] with the work of Zdyrski and Feddersen [47], and construct a dynamical model for the interaction of Stokes waves with a turbulent wind, thereby including weak non-linear effects in both air and water. This is a way to account for the feedback of the waves on the wind.

7. Appendix

When I'm walking a dark road, I am a man who walks alone.
– **Iron Maiden**, Fear of the Dark, 1992.

Here is a set of useful formulae involving a velocity field, $\boldsymbol{u}$, and the corresponding vorticity field, $\boldsymbol{\omega} = \nabla \times \boldsymbol{u}$. We do not assume incompressibility.

1. Convective acceleration:

$$(\boldsymbol{u} \cdot \nabla)\boldsymbol{u} = \frac{1}{2}\nabla|\boldsymbol{u}|^2 + \boldsymbol{\omega} \times \boldsymbol{u} \tag{7.1}$$

2. Laplacian:

$$\nabla^2 \boldsymbol{u} = \nabla(\nabla \cdot \boldsymbol{u}) - \nabla \times \boldsymbol{\omega} \tag{7.2}$$

3. Gradient property for any scalar field φ:

$$\nabla(\varphi \boldsymbol{u}) = \boldsymbol{u} \cdot \nabla\varphi + (\nabla \cdot \boldsymbol{u})\varphi \tag{7.3}$$

4. Divergence of the cross product:

$$\nabla \cdot (\boldsymbol{\omega} \times \boldsymbol{u}) = |\boldsymbol{\omega}|^2 - \boldsymbol{u} \cdot (\nabla \times \boldsymbol{\omega}) \tag{7.4}$$

5. Curl of the cross product:

$$\nabla \times (\boldsymbol{\omega} \times \boldsymbol{u}) = (\nabla \cdot \boldsymbol{u})\boldsymbol{\omega} - (\nabla \cdot \boldsymbol{\omega})\boldsymbol{u} + (\boldsymbol{u} \cdot \nabla)\boldsymbol{\omega} - (\boldsymbol{\omega} \cdot \nabla)\boldsymbol{u} \tag{7.5}$$

References

[1] P. A. E. M. JANSSEN. *The Interaction of Ocean Waves and Wind*. Cambridge University Press, Cambridge, UK, 2004. 23, 57

[2] L. CAVALERI, B. FOX-KEMPER, AND M. HEMER. **Wind Waves in the Coupled Climate system**. *Bull. Am. Met. Soc.*, **93**(11):1651–1661, 2012. 23

[3] D. RICHTER AND F. VERON. **Ocean spray: An outsized influence on weather and climate**. *Physics Today*, **69**(11):35–39, 2016. 23

[4] **Scientific Background on the Nobel Prize in Physics 2021**. 23

[5] W. J. PIERSON AND L. MOSKOWITZ. **A proposed spectral form for fully developed wind seas based on the similarity theory of S.A. Kitaigorodskii**. Technical report, US Naval Oceanographic Office, 1963. 23

[6] O. M. PHILLIPS. **On the generation of waves by turbulent wind**. *J. Fluid Mech.*, **2**:417–445, 1957. 23

[7] T. LI AND L. SHEN. **The principal stage in wind-wave generation**. *J. Fluid Mech.*, **934**:A41, 2022. 23

[8] A. D. D. CRAIK. **The Origins of Water Wave Theory**. *Annu. Rev. Fluid Mech.*, **36**:1–28, 2004. 24

[9] G. B. AIRY. **Tides and waves**. *Encyclopaedia Metropolitana*, **Vol. 3**, 1841. 24

[10] O. BÜHLER. *Waves and mean flows*. Cambridge University Press, 2014. 24

[11] E. VAN SEBILLE ET AL. **The physical oceanography of the transport of floating marine debris**. *Environ. Res. Lett.*, **15**:023003, 2020. 24

[12] M. CHAMECKI, T. CHOR, D. YANG, AND C. MENEVEAU. **Material Transport in the Ocean Mixed Layer: Recent Developments Enabled by Large Eddy Simulations**. *Rev. Geophys.*, **57**:1338–1371, 2019. 24

[13] J. W. MILES. **On the generation of surface waves by shear flows**. *J. Fluid Mech.*, **3**:185–204, 1957. 24, 25, 55, 56, 57

[14] M. J. W. LIGHTHILL. **Physical interpretation of the mathematical theory of wave generation by wind**. *J. Fluid Mech.*, **14**:385–398, 1962. 24, 56

[15] J. W. MILES. **Surface-wave generation revisited**. *J. Fluid Mech.*, **256**:427–441, 1993. 24

[16] J. R. CARPENTER, M. P. BUCKLEY, AND F. VERON. **Evidence of the critical layer mechanism in growing wind waves**. *J. Fluid Mech.*, **948**:A26, 2022. 25, 57

[17] J. WU, S. POPINET, AND L. DEIKE. **Revisiting wind wave growth with fully coupled direct numerical simulations**. *J. Fluid Mech.*, **951**:A18, 2022. 25, 57

[18] W. R. Young and C. L. Wolfe. **Generation of surface waves by shear flow instabilities**. *J. Fluid Mech.*, **739**:276–307, 2014. 25, 60, 61, 62

[19] O. M. Phillips. **On the dynamics of unsteady gravity waves of finite amplitude. Part I. The elementary interactions**. *Journal of Fluid Mechanics*, **9**:193–217, 1960. 25

[20] K. Hasselmann. **On the non-linear energy transfer in a gravity-wave spectrum Part 1. General theory**. *J. Fluid Mech.*, **12**:481 – 500, 1962.

[21] V. E. Zakharov. **Stability of periodic waves of finite amplitude on the surface of a deep fluid**. *J. Appl. Mech. Tech. Phys.*, **9**:190–194, 1968. 25

[22] A. I. Dyachenko, D. I. Kachulin, and V. E. Zakharov. **Super compact equation for water waves**. *J. Fluid Mech.*, **828**:661 – 679, 2017. 25

[23] S. Nazarenko. *Wave Turbulence*. Lecture Notes in Physics. Springer, 2011. 25

[24] P. A. E. M. Janssen. *The wave model*. ECMWF, 2002. 26

[25] Z. Hani Y. Deng. **Full derivation of the wave kinetic equation**. *arXiv:2104.11204*, 2021. 26

[26] L. E. Reichl and M-B. Tran. **A kinetic equation for ultra-low temperature Bose–Einstein condensates**. *J. Phys. A: Math. Theor*, **52**:063001, 2019. 26

[27] Y. Onuki, J. Guioth, and F. Bouchet. **Dynamical large deviations for an inhomogeneous wave kinetic theory: linear wave scattering by a random medium**. *arXiv:2301.03257*, 2023. 26

[28] H. Jeffreys. **On the formation of water waves by wind**. *Proc. R. Soc. Lond. A*, **107**:189–206, 1925. 27, 60, 61

[29] P. G. Drazin and W. H. Reid. *Hydrodynamic stability*. Cambridge University Press, 1981. 29, 33

[30] S. Chandrasekhar. *Hydrodynamic and Hydromagnetic Stability*. Oxford University Press, 1961. 29

[31] P. Huerre and M. Rossi. *Hydrodynamics and Nonlinear Instabilities*, chapter 2: Hydrodynamic instabilities in open flows. Cambridge University Press, 2005. 33

[32] H. B. Squire. **On the Stability for Three-Dimensional Disturbances of Viscous Fluid Flow between Parallel Walls**. *Proc. R. Soc. Lond. A*, **142**:621–628, 1933. 35

[33] C. C. Lin. *The Theory of Hydrodynamic Stability*. Cambridge University Press, 1955. 35, 40, 56, 66

[34] C. M. Bender and S. A. Orszag. *Advanced Mathematical Methods for Scientists and Engineers*. Springer, 1999. 38, 59

[35] W. Heisenberg. **Über Stabilität and Turbulenz von Flüssigkeitsströmen**. *Annalen der Physik*, **379**(577-627), 1924. 38

[36] W. Tollmien. **Über die Entstehung der Turbulenz**. *Nachr. Ges. Wiss. Göttingen, Math.-phys. Kl.*, pages 21–44, 1929. 39

[37] P. H. LeBlond and L. A. Mysak. *Waves in the ocean*. Elsevier Science, 1981. 45

[38] Lord Rayleigh. **Investigation of the character of the equilibrium of an incompressible heavy fluid of variable density**. *Proc. Lond. Math. Soc.*, **14**:170–177, 1883. 51

[39] Sir G. I. Taylor. **The instability of liquid surfaces when accelerated in a direction perpendicular to their planes**. *Proc. R. Soc. Lond. A*, **201**:192–196, 1950. 51

[40] S. D. CONTE AND J. W. MILES. **On the numerical integration of the Orr-Sommerfeld equation**. *J. Soc. Indust. App. Math.*, **7**:361–366, 1959. 57

[41] A. S. MONIN AND A. M. YAGLOM. *Statistical Fluid Mechanics, Volume I: Mechanics of Turbulence*. MIT Press, Cambridge, Massachusetts, 1971. 57

[42] T. H. HUGHES AND W. H. REID. **On the stability of the asymptotic suction boundary-layer profile**. *J. Fluid Mech.*, **23**:717–735, 1965. 57

[43] S. BEJI AND K. NADAOKA. **Solution of Rayleigh's instability equation for arbitrary wind profiles**. *J. Fluid Mech.*, **500**:65–73, 2004. 58

[44] L. C. MORLAND AND P. G. SAFFMAN. **Effect of wind profile on the instability of wind blowing over water**. *J. Fluid Mech.*, **252**:383–398, 1992. 58

[45] A. ALEXAKIS, Y. YOUNG, AND R. ROSNER. **Weakly nonlinear analysis of wind-driven gravity waves**. *J. Fluid Mech.*, **503**:171–200, 2004. 62

[46] P. A. E. M. JANSSEN. **Quasilinear approximation for the spectrum of wind-generated water waves**. *J. Fluid Mech.*, **117**:493–506, 1982. 67

[47] T. ZDYRSKI AND F. FEDDERSEN. **Wind-induced changes to surface gravity wave shape in deep to intermediate water**. *J. Fluid Mech.*, **903**:A31, 2020. 67